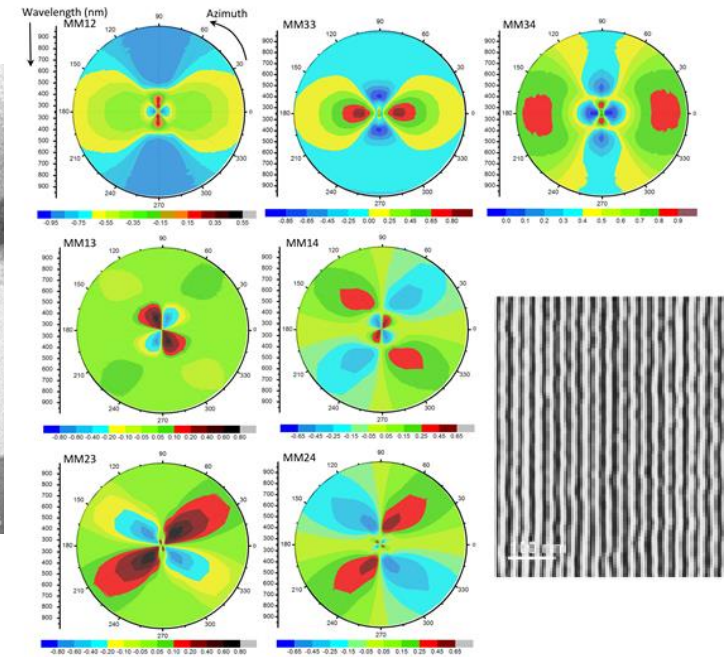
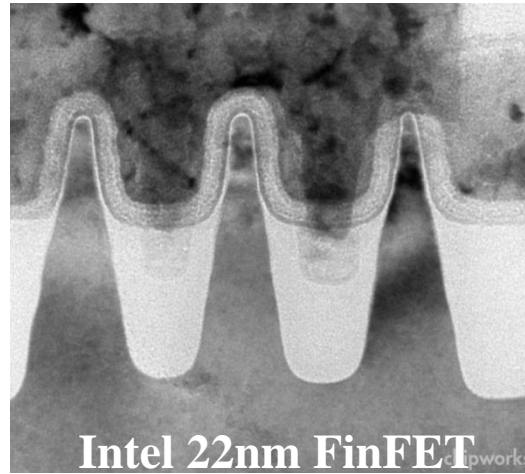
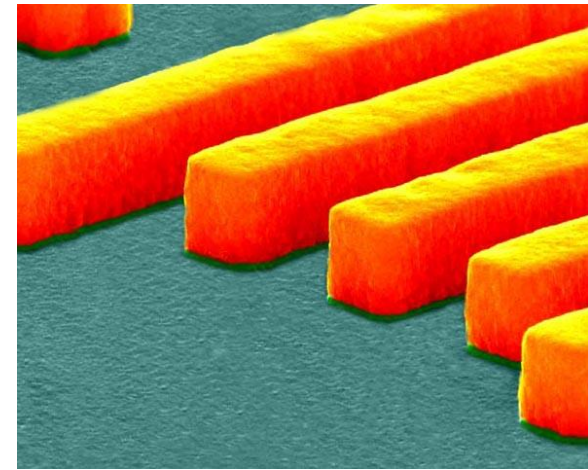


**SUNY** POLYTECHNIC  
INSTITUTE

MULLER MATRIX SPECTROSCOPIC ELLIPSOMETRY  
BASED SCATTEROMETRY

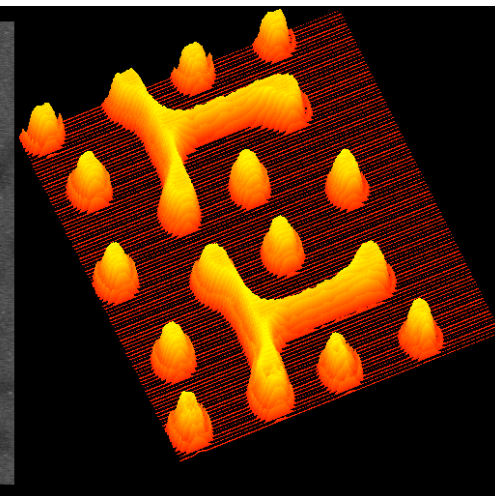
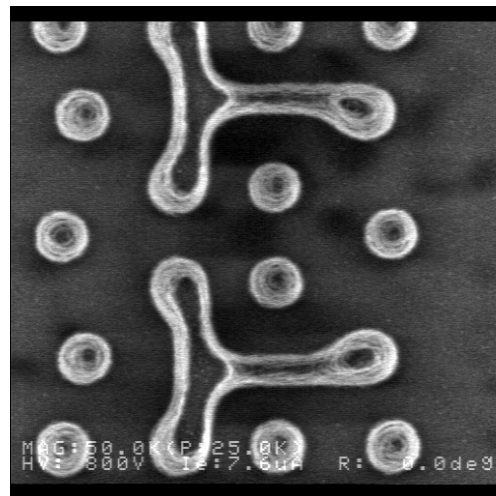
**Alain C. Diebold**

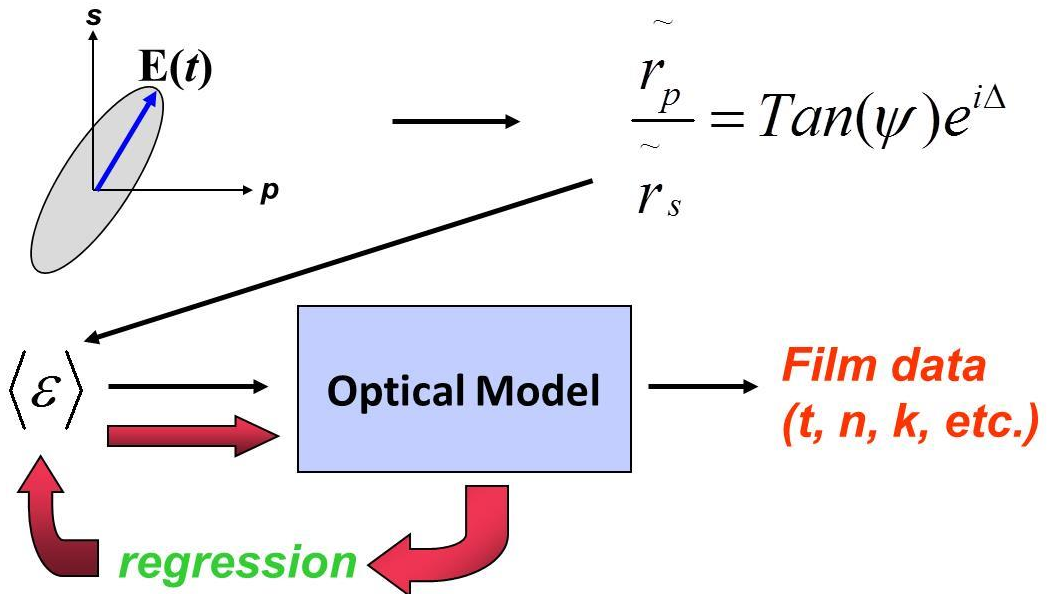
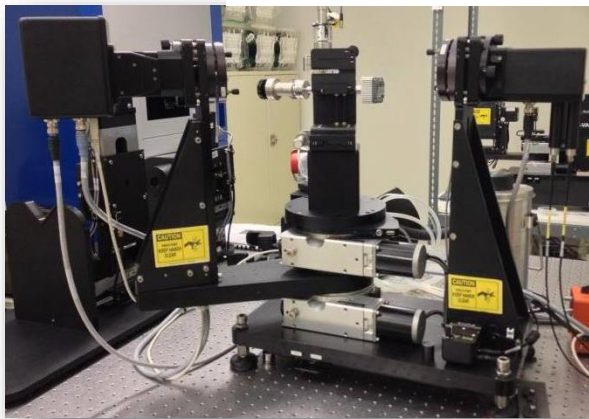
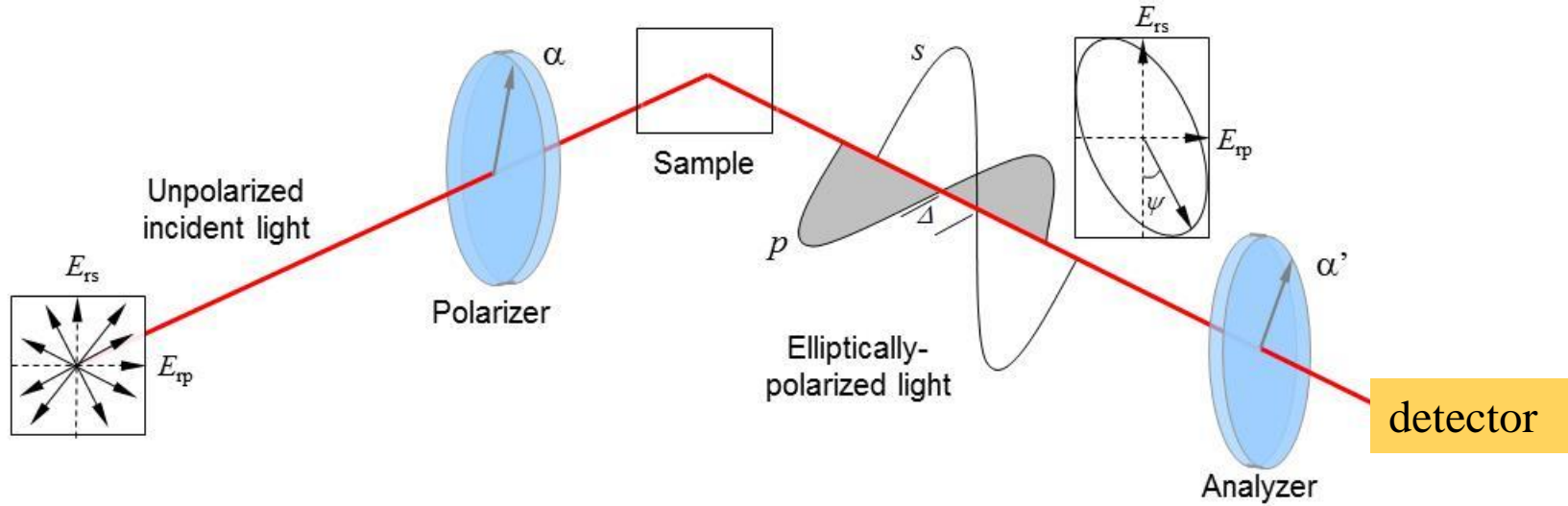
- Introduction
- Mueller Matrix Spectroscopic Ellipsometry
- Simulation Methods
  - Rigorous Coupled Wave Analysis (RCWA)
- Scatterometry of Fins
- Scatterometry of DSA BCP
- Scatterometry of Copper Cross-Grating
- Conclusions



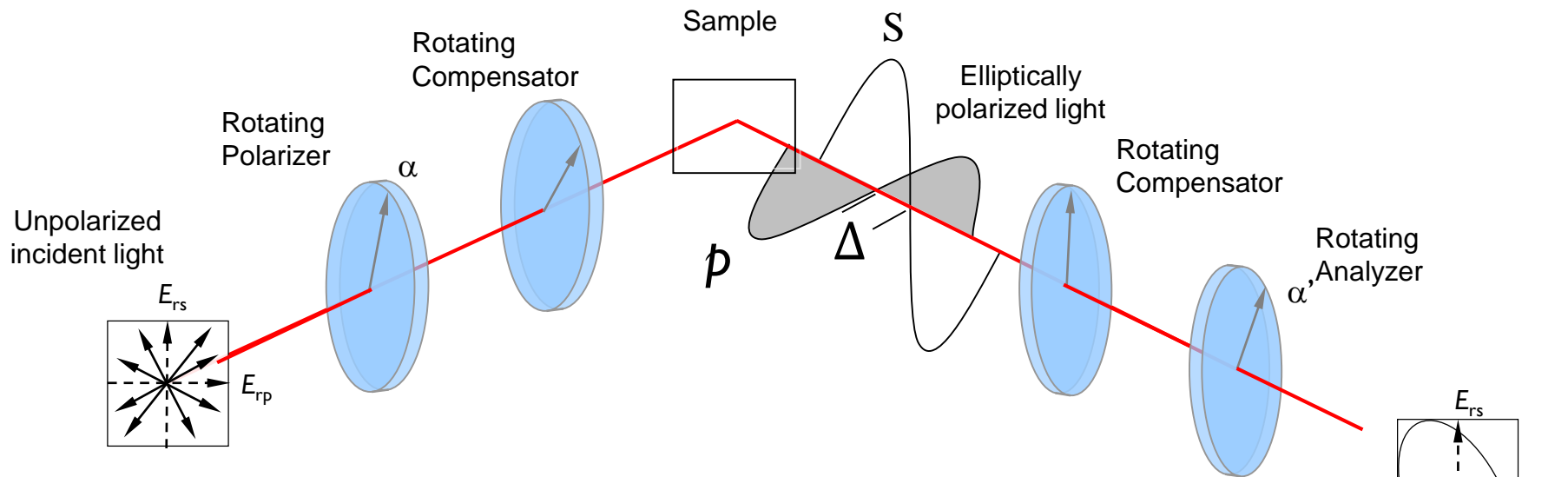
**Scatterometry measurement of  
of shape profile with dimensional  
Information  
Is an alternative to CD-SEM**

Figures : Andras Vladar (NIST) and  
Synopsis & A.C. Diebold – SPIE Key  
Note 2011





## Laboratory Ellipsometer Great for All Types of Samples

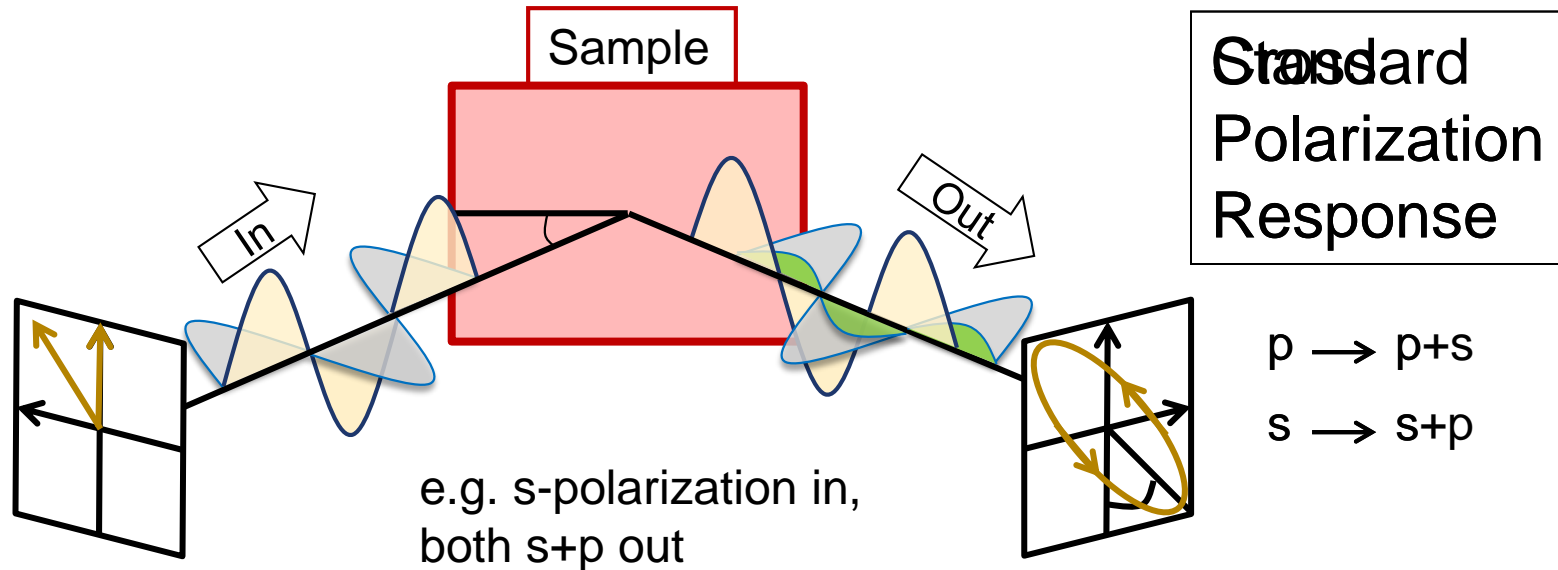


$$S = \begin{bmatrix} s_0 \\ s_1 \\ s_2 \\ s_3 \end{bmatrix} = \begin{bmatrix} I_x + I_y \\ I_x - I_y \\ I_{\pi/4} - I_{-\pi/4} \\ I_{LCP} - I_{RCP} \end{bmatrix}$$

Stokes Vector

$$\begin{bmatrix} S_{0,out} \\ S_{1,out} \\ S_{2,out} \\ S_{3,out} \end{bmatrix} = \begin{bmatrix} M_{11} & M_{12} & M_{13} & M_{14} \\ M_{21} & M_{22} & M_{23} & M_{24} \\ M_{31} & M_{32} & M_{33} & M_{34} \\ M_{41} & M_{42} & M_{43} & M_{44} \end{bmatrix} \begin{bmatrix} S_{0,in} \\ S_{1,in} \\ S_{2,in} \\ S_{3,in} \end{bmatrix}$$

Mueller Matrix



- Isotropic samples
  - ▣ Refractive indices of thin films lack spatial dependence
  - ▣ Thus, no azimuthal dependence or cross-polarization
- Anisotropic structures
  - ▣ Patterned surfaces result in spatially varying refractive indices
  - ▣ Thus, azimuthal dependence reflects sample symmetry

Anisotropic, generalizing

Post-normalization

$$M = \begin{pmatrix} M_{11} & M_{12} & M_{13} & M_{14} \\ M_{21} & M_{22} & M_{23} & M_{24} \\ M_{31} & M_{32} & M_{33} & M_{34} \\ M_{41} & M_{42} & M_{43} & M_{44} \end{pmatrix} \Downarrow = \begin{pmatrix} 1 & -N - \alpha_{sp} & C_{sp} + \zeta_1 & S_{sp} + \zeta_2 \\ -N - \alpha_{ps} & 1 - \alpha_{sp} - \alpha_{ps} & -C_{sp} + \zeta_1 & -S_{sp} + \zeta_2 \\ C_{ps} + \xi_1 & -C_{ps} + \xi_1 & C_{pp} + \beta_1 & S_{pp} + \beta_2 \\ -S_{ps} + \xi_2 & S_{ps} + \xi_2 & -S_{pp} - \beta_2 & C_{pp} + \beta_1 \end{pmatrix}$$

- Matrix contains complete optical response of a sample
- Symmetry reduces number of independent elements
- 15 distinct elements in general

$$D = 1 + \tan^2(\psi_{pp}) + \tan^2(\psi_{ps}) + \tan^2(\psi_{sp})$$

$$N = \frac{1 - \tan^2(\psi_{pp}) - \tan^2(\psi_{ps}) - \tan^2(\psi_{sp})}{D}$$

$$C_{ij} = \frac{2 \tan(\psi_{ij}) \cos \Delta_{ij}}{D}$$

$$S_{ij} = \frac{2 \tan(\psi_{ij}) \sin \Delta_{ij}}{D}$$

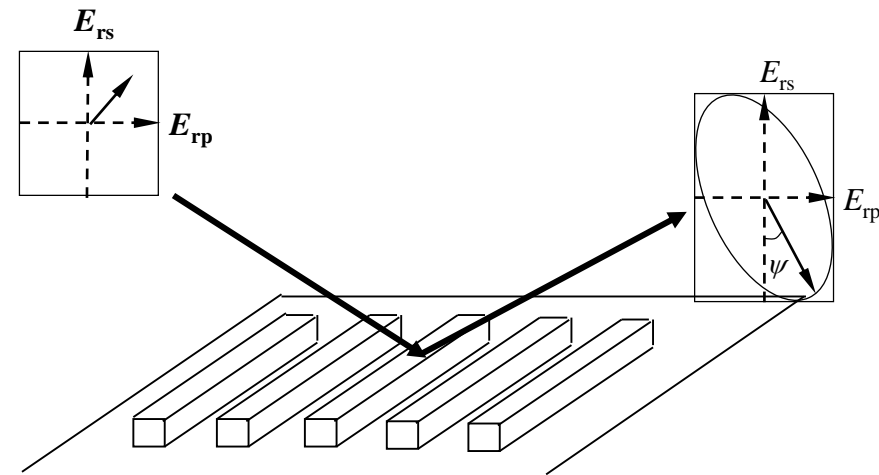
$$\alpha_{ij} = \frac{2 \tan^2(\psi_{ij})}{D}$$

$$\zeta_i = \frac{D (C_{ps}^2 + S_{ps}^2 (-1)^{i+1 \bmod 2})}{2}$$

$$\xi_i = \frac{D (C_{sp}^2 + S_{sp}^2 (-1)^{i+1 \bmod 2})}{2}$$

$$\beta_i = \frac{D (C_{sp} C_{ps} + S_{sp} S_{ps} (-1)^{i+1 \bmod 2})}{2}$$

- Inline optical metrology tool for critical dimension (CD) measurement for advanced process control.
- Fast, accurate & non-destructive.
- Diffraction from a periodic grating.
- **Optical simulator is used to generate the optical response for the structure of interest (Forward problem) and regression based or library based approach is used to extract the feature dimensions/additional information (Reverse problem).**



**Ellipsometry of Grating Structures**

$$\tan \Psi e^{j\Delta} = \frac{R^p}{R^s}$$

Ellipsometric Response

Optical Response

$$\begin{pmatrix} S_{0,\text{out}} \\ S_{1,\text{out}} \\ S_{2,\text{out}} \\ S_{3,\text{out}} \end{pmatrix} = \begin{pmatrix} M_{11} & M_{12} & M_{13} & M_{14} \\ M_{21} & M_{22} & M_{23} & M_{24} \\ M_{31} & M_{32} & M_{33} & M_{34} \\ M_{41} & M_{42} & M_{43} & M_{44} \end{pmatrix} \begin{pmatrix} S_{0,\text{in}} \\ S_{1,\text{in}} \\ S_{2,\text{in}} \\ S_{3,\text{in}} \end{pmatrix}$$

Mueller Response

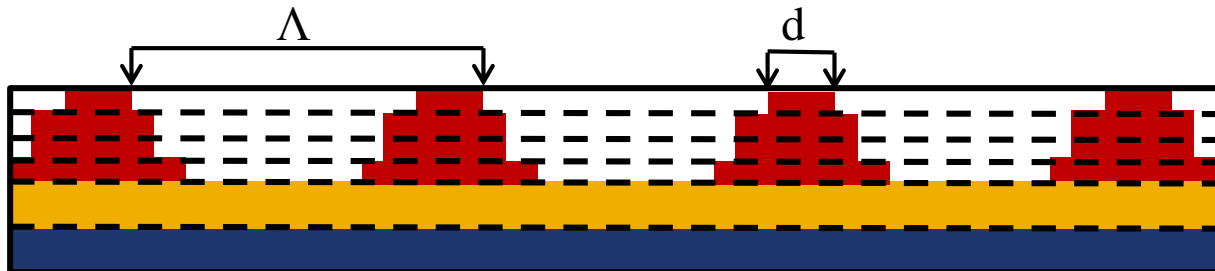


- Approximate full Fourier series for dielectric function

$$\epsilon(x) = \sum_{n=-N}^N \hat{a}_n e^{i2\pi n x / L}$$

- Slice structure into stack of layers, coefficients determined:

$$\epsilon_{n=0} = \epsilon_{line} d / L + \epsilon_{space} (1 - d / L) \quad \epsilon_{n \neq 0} = (\epsilon_{line} - \epsilon_{space}) \sin(\pi n d / L) / \pi n$$



- Solve Maxwell's equations for incident TM polarized waves

$$\nabla^2 E_y(x, z) + k_z^2 E_y(x, z) = \sum_{m=-\infty}^{\infty} \hat{a}_m e^{i(k_x m x + k_z z)}$$

The interaction of light with the optical elements of the ellipsometer and the sample can be represented by the **Mueller matrix (MM) Transformation**.

The intensity & polarization of the light can be represented by a **Stokes vector**

$$\begin{matrix} \hat{e} \\ \hat{e} \\ \hat{e} \\ \hat{e} \\ \hat{e} \end{matrix} \begin{matrix} I_x + I_y \\ I_x - I_y \\ I_{45} - I_{-45} \\ I_L - I_R \end{matrix} \begin{matrix} \hat{u} \\ \hat{u} \\ \hat{u} \\ \hat{u} \\ \hat{u} \end{matrix} \begin{matrix} S_{0,\text{out}} \\ S_{1,\text{out}} \\ S_{2,\text{out}} \\ S_{3,\text{out}} \end{matrix} = \begin{pmatrix} M_{11} & M_{12} & M_{13} & M_{14} \\ M_{21} & M_{22} & M_{23} & M_{24} \\ M_{31} & M_{32} & M_{33} & M_{34} \\ M_{41} & M_{42} & M_{43} & M_{44} \end{pmatrix} \begin{matrix} S_{0,\text{in}} \\ S_{1,\text{in}} \\ S_{2,\text{in}} \\ S_{3,\text{in}} \end{matrix}$$

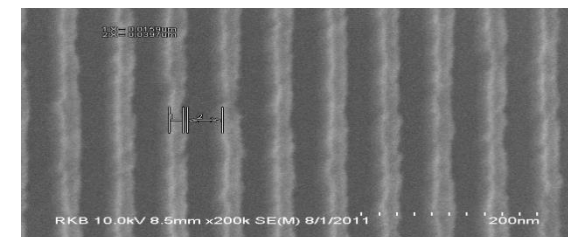
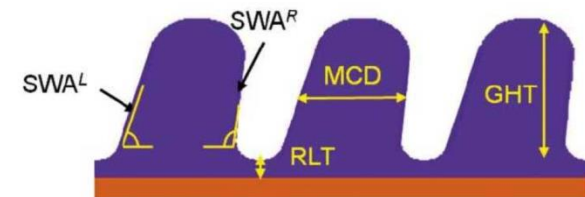
Why does this matter?

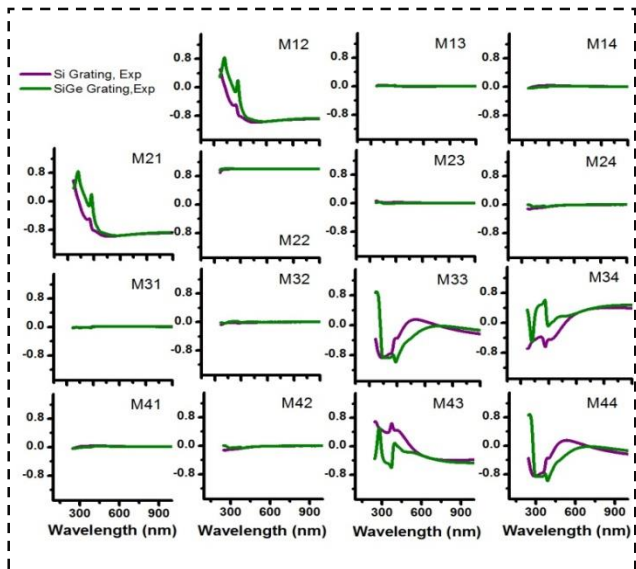
If you have samples with asymmetry/anisotropy

If you have samples that depolarize—roughness, systematic errors

The full generalized MM description gives complete information about the sample.

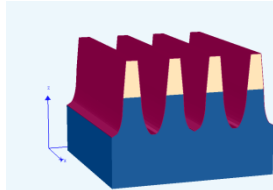
**Anisotropy in off-diagonal elements and depolarization is distributed among the Mueller matrix elements**



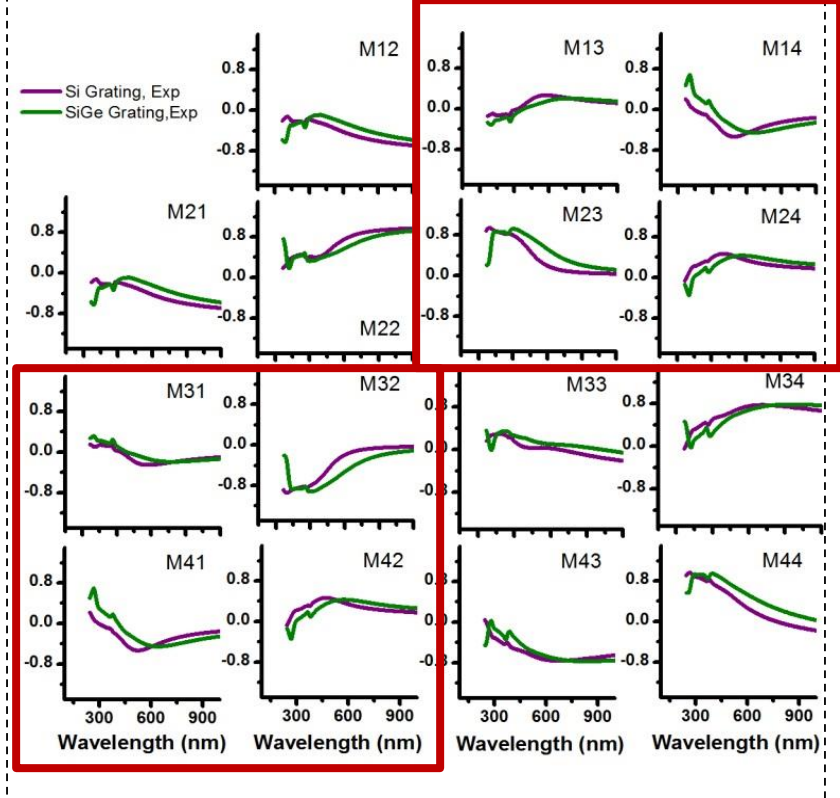
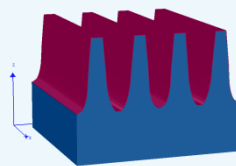


**Azimuth = 0°**

**SiGe Grating**



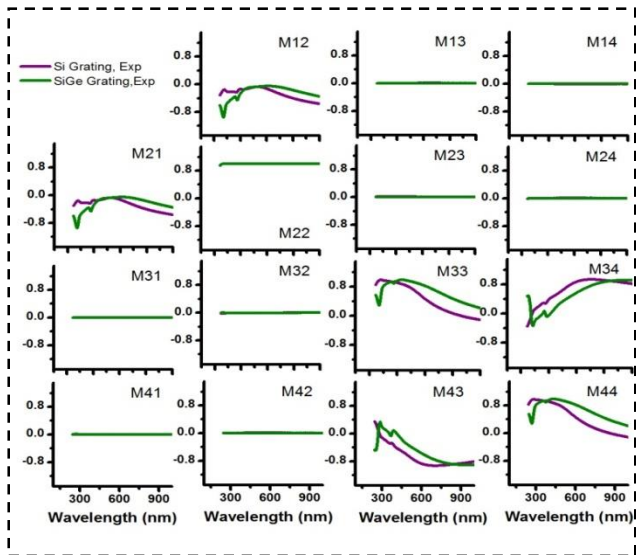
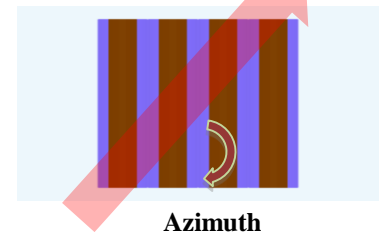
**Si Grating**



**Azimuth = 45°**

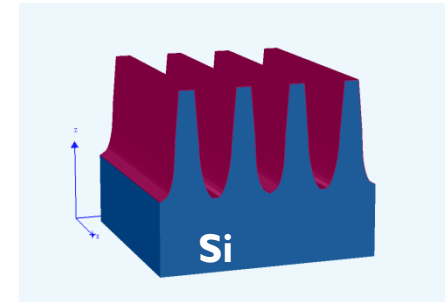
Non-zero off-diagonal  
Mueller response

**Top View**

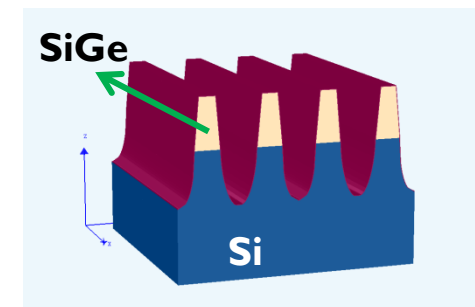


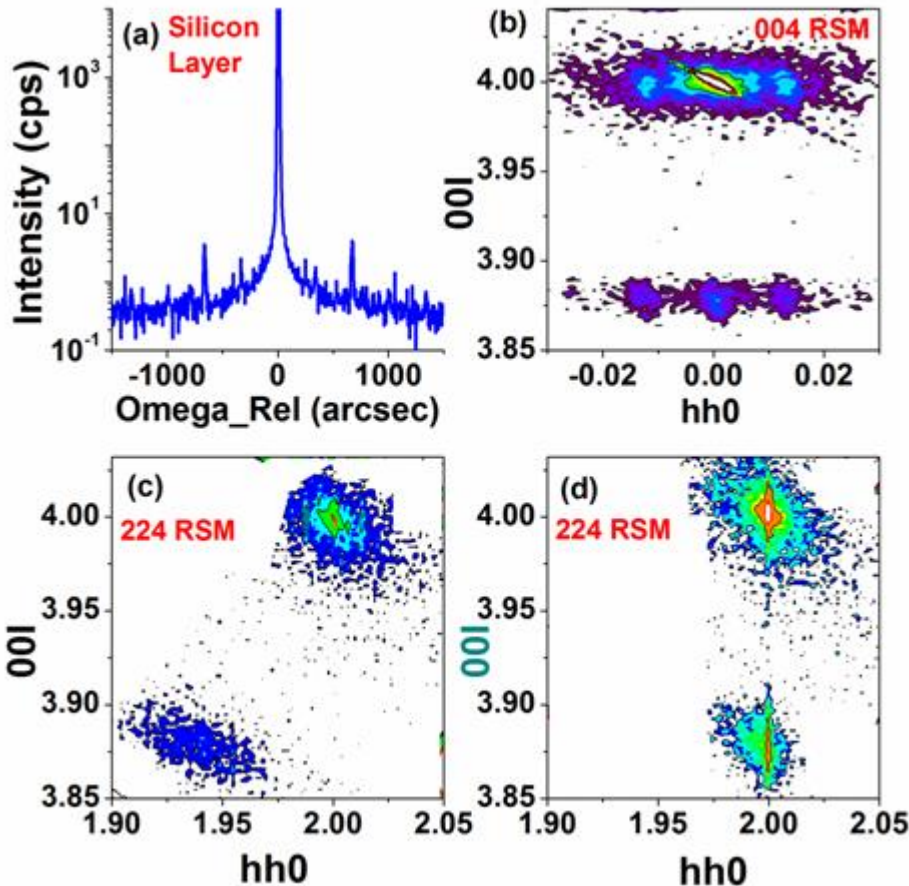
**Azimuth = 90°**

Wafer ID	Si Fins			Coupled Multi-azimuth Regression
Mean OCD values	Azimuth			
	0°	45°	90°	
Bottom CD (nm)	29.3 $1\sigma=0.01$	32.4 $1\sigma=0.01$	31.3 $1\sigma=0.03$	30.9
Top CD (nm)	11.7 $1\sigma=0.01$	12.7 $1\sigma=0.01$	12.3 $1\sigma=0.01$	11.4
Height (nm)	65.5 $1\sigma=0.07$	66.3 $1\sigma=0.02$	67.5 $1\sigma=0.01$	65.9
MSE	0.03	0.06	0.04	0.04



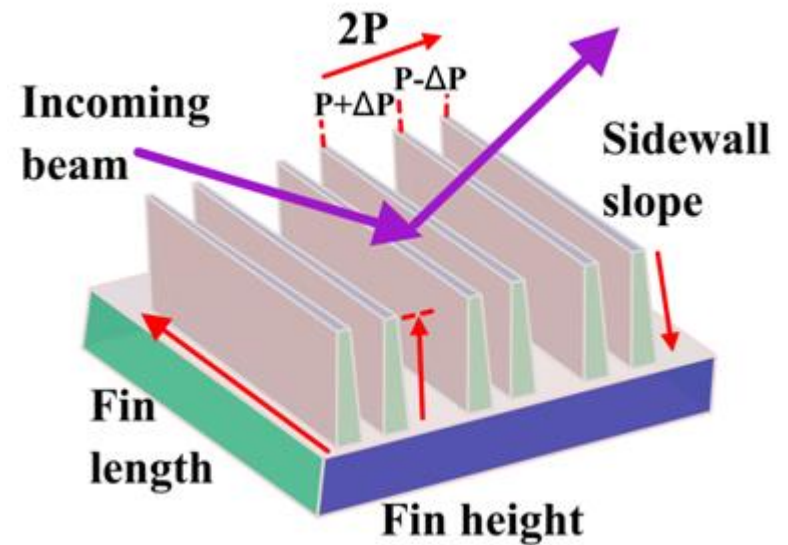
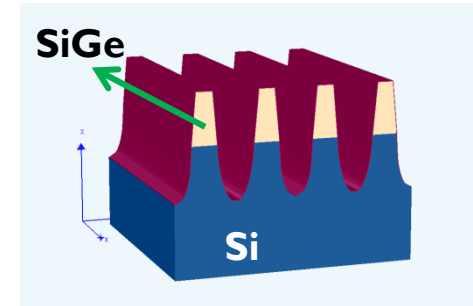
Wafer ID	SiGe Fins			Coupled Multi-azimuth Regression
Mean OCD values	Azimuth			
	0°	45°	90°	
Bottom CD (nm)	24.2 $1\sigma=0.03$	29.2 $1\sigma=0.03$	26.2 $1\sigma=0.02$	24.5 $1\sigma=0.03$
Top CD (nm)	11.8 $1\sigma=0.01$	14.6 $1\sigma=0.01$	12.1 $1\sigma=0.01$	14.8 $1\sigma=0.01$
SiGe Height (nm)	35.1 $1\sigma=0.02$	35.3 $1\sigma=0.03$	36.2 $1\sigma=0.03$	36.7 $1\sigma=0.02$
MSE	0.09	0.18	0.06	0.15





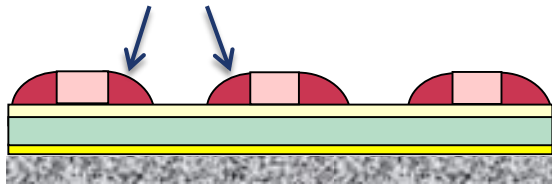
**Beam  $\perp$  to Fins**

**Beam  $\parallel$  to Fins**

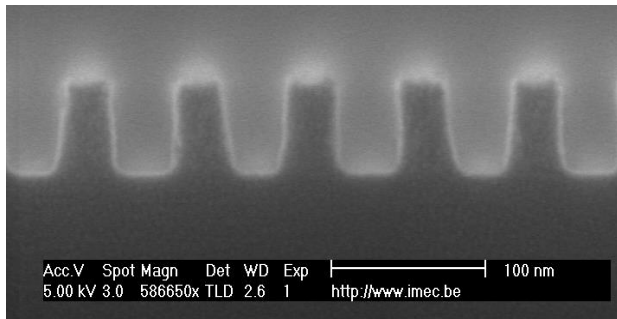
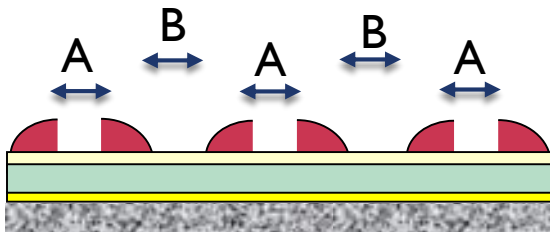


SiGe layer strained along the length of the fin and partially relaxed perpendicular to it.

Spacer Pattern

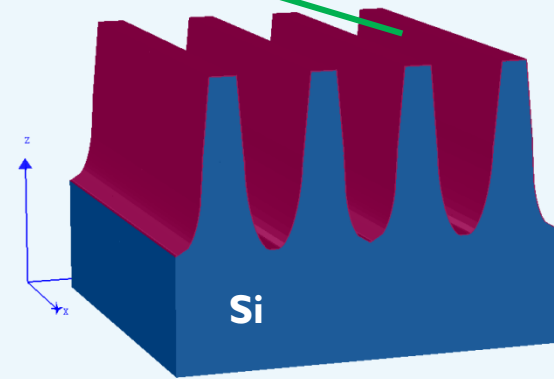


Two space distances = pitch walking



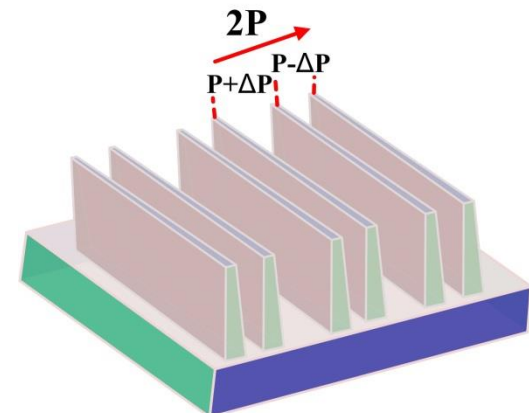
No Pitch Walking

Surface oxide

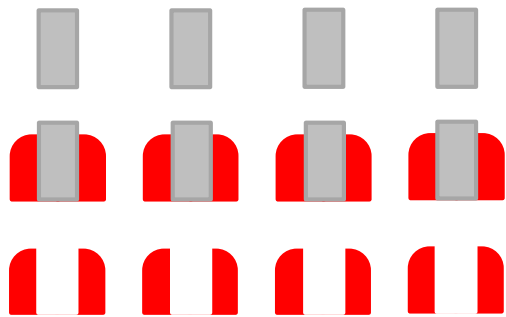


Pitch Walking

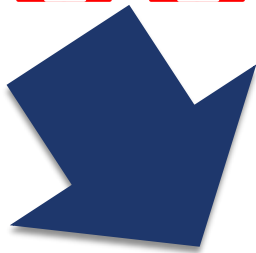
~ 1nm pitch difference plus uneven etching



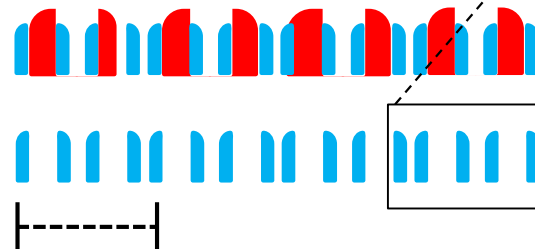
## 1<sup>st</sup> Spacer Patterning



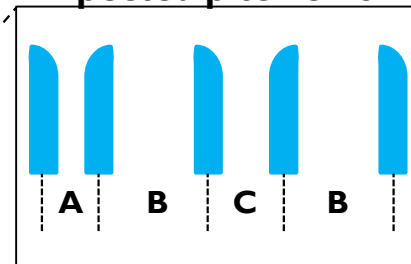
**3 Space Values instead of 2**



## 2<sup>nd</sup> Spacer Patterning



Expected pitch error



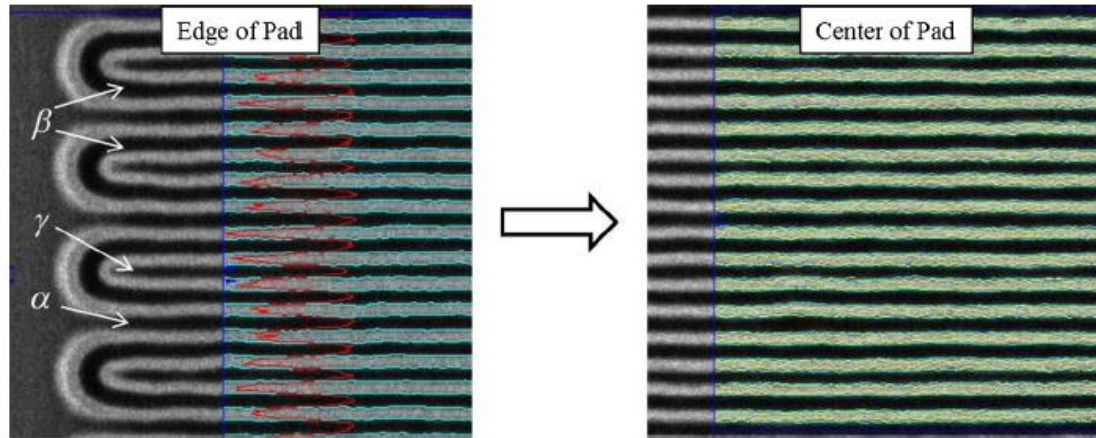
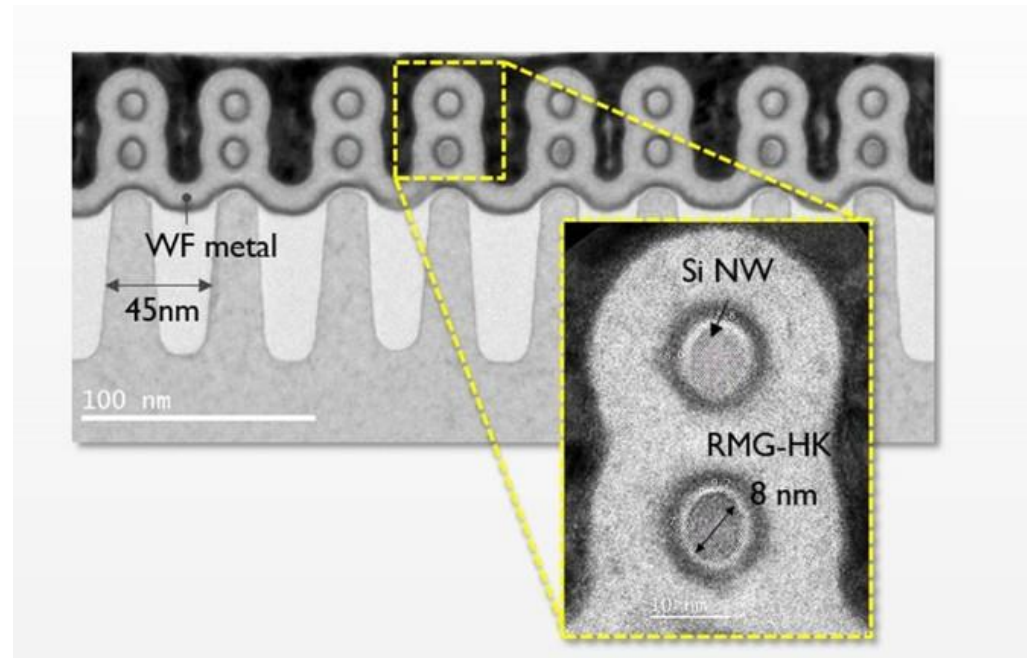
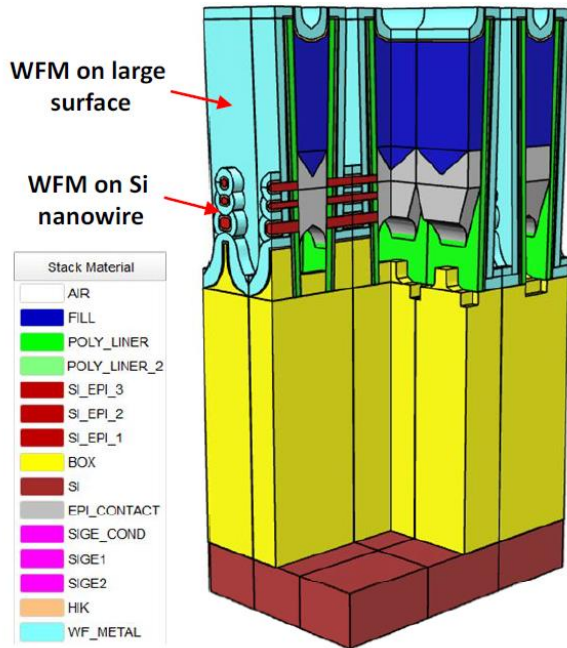


Fig. 4 The CD-SEM would locate  $\alpha$ ,  $\beta$ , and  $\gamma$  on the edge of OCD measurement pad and jump to center of pad.

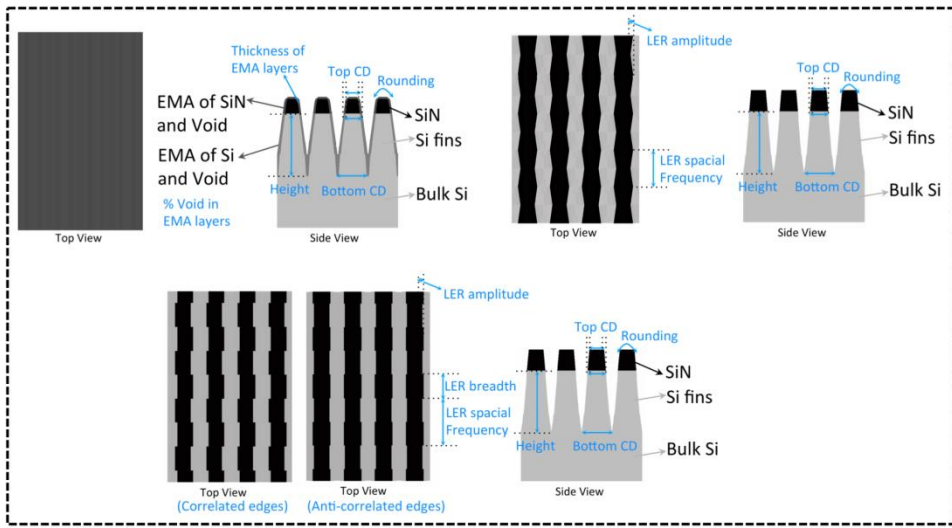
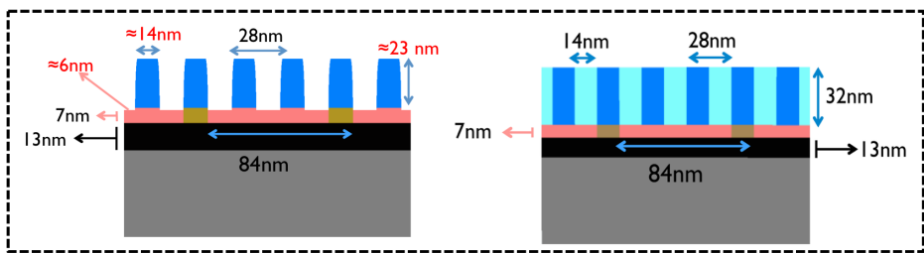
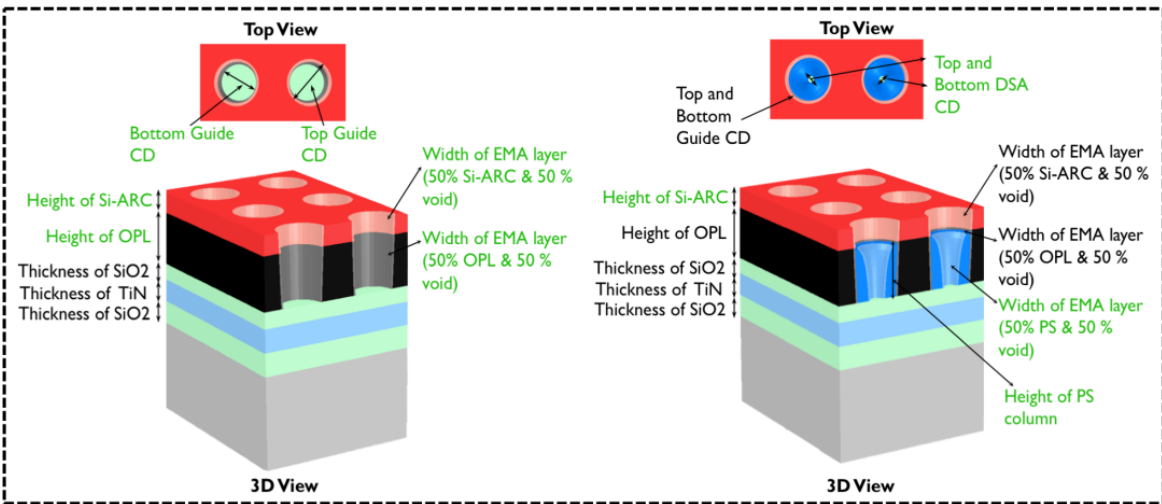
**2 nm Improvement in measurement in Stability  
of Measurement of Pitch Walking using Virtual Referencing**

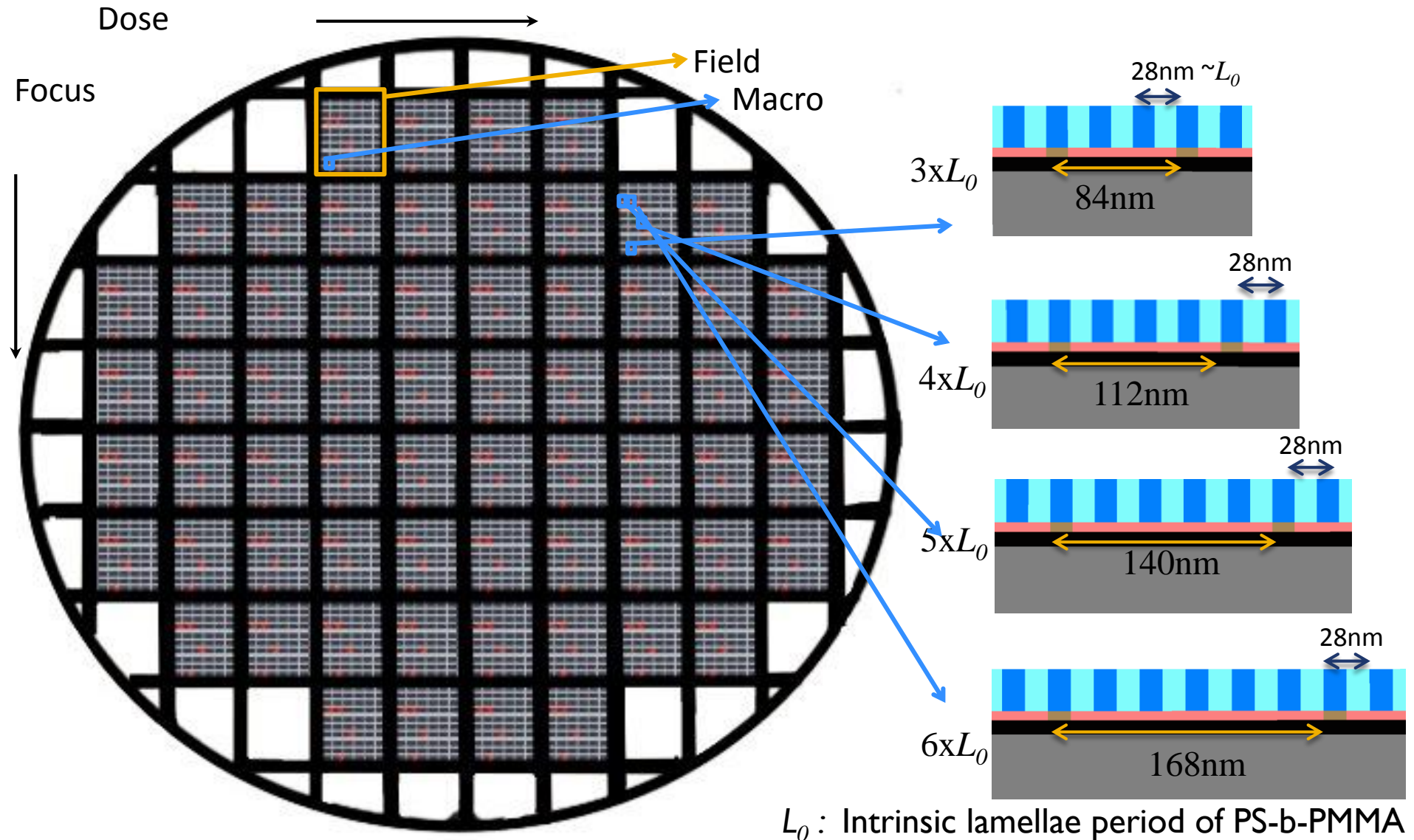
Taher Kagalwala, Alok Vaid, et al, J. Micro/Nanolith. MEMS MOEMS 15(4), 044004 (2016)



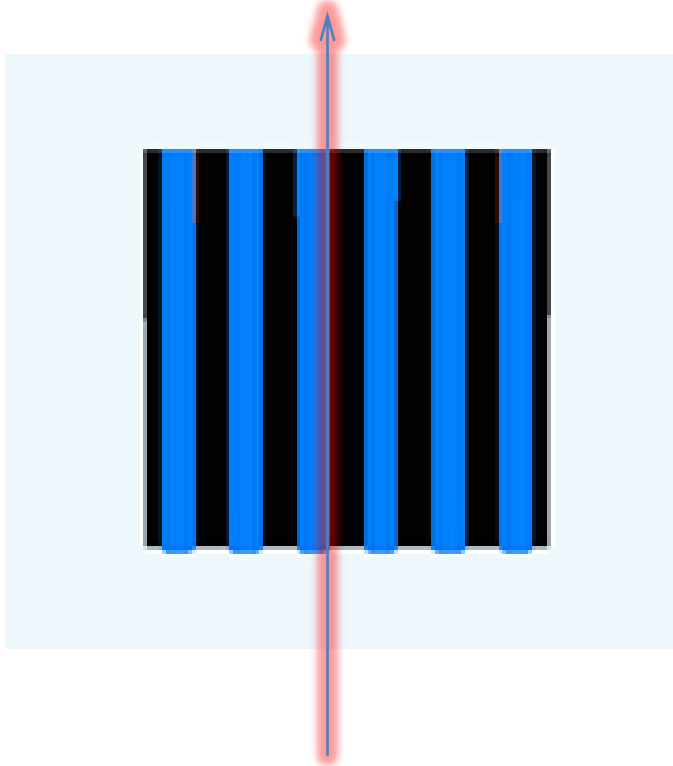


- Advanced in-line optical metrology of sub-10nm structures for gate all around devices (GAA), R. Muthinti, SPIE 2016 – **Scatterometry**
- Vertically Stacked Gate-All-Around Si Nanowire CMOS Transistors with Dual Work Function Metal Gates, H. Mertens, et al, (IEDM 2016)

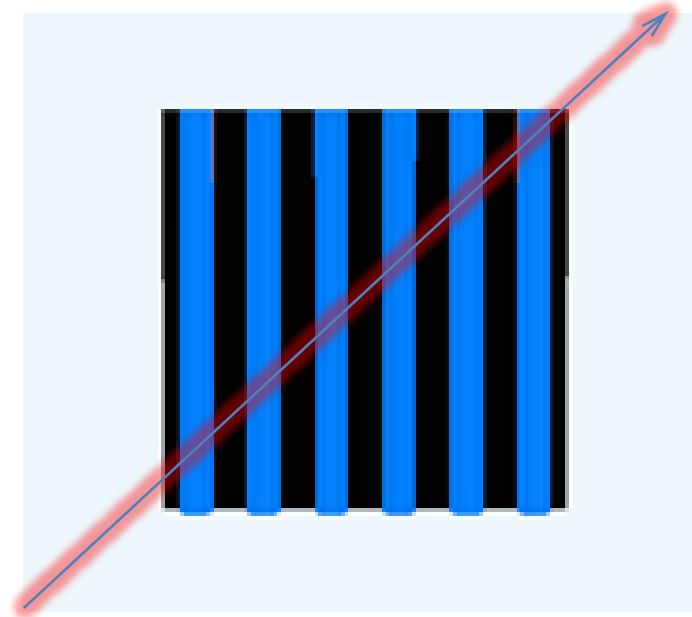


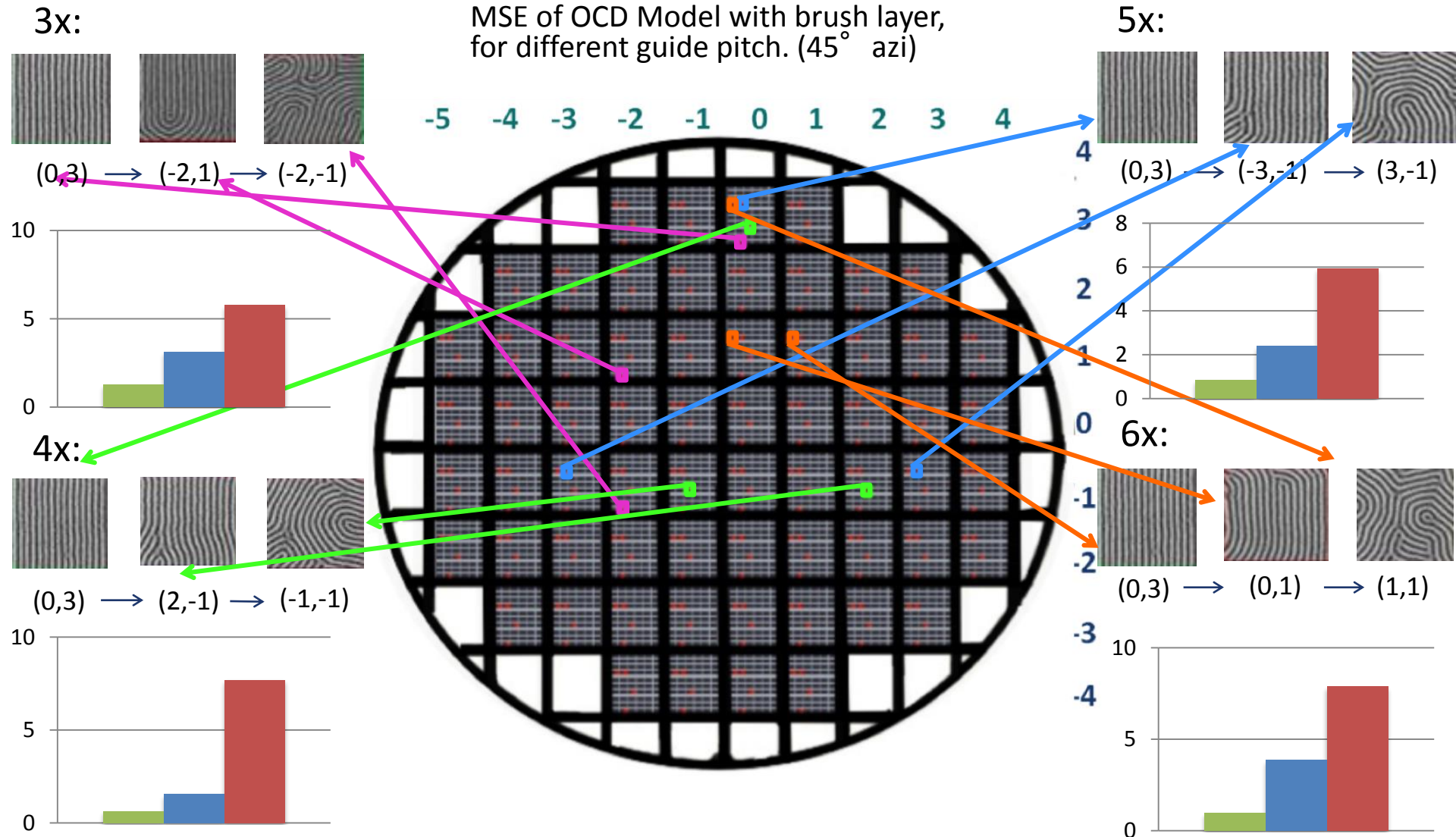


Azimuth  $90^\circ$



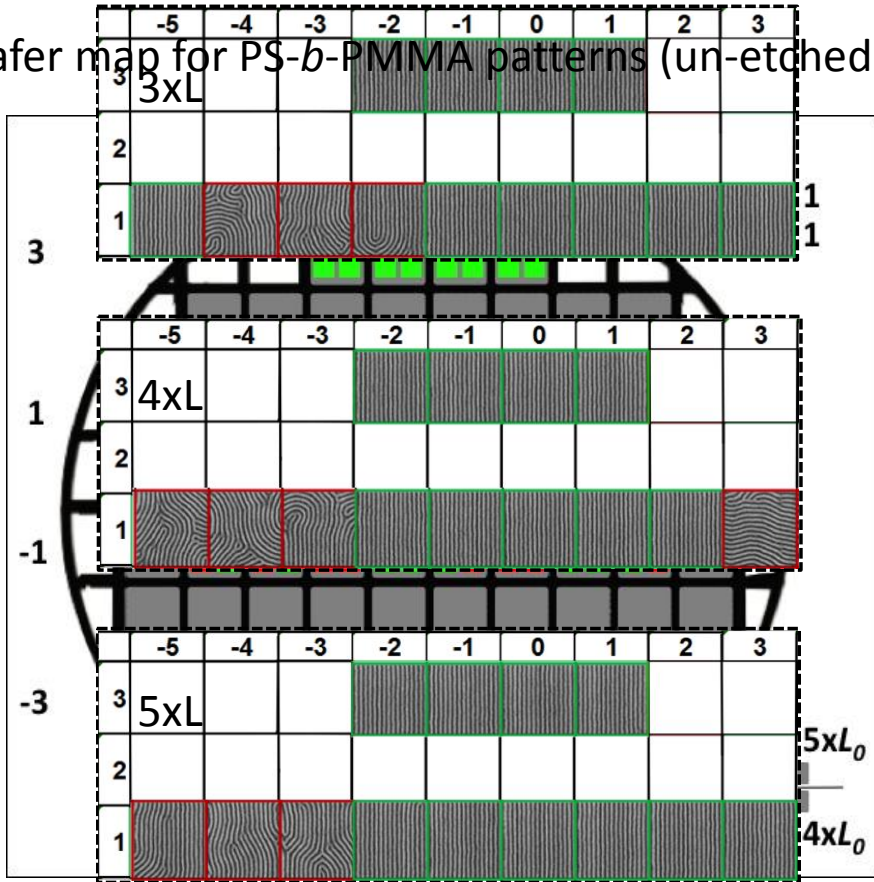
Azimuth  $45^\circ$



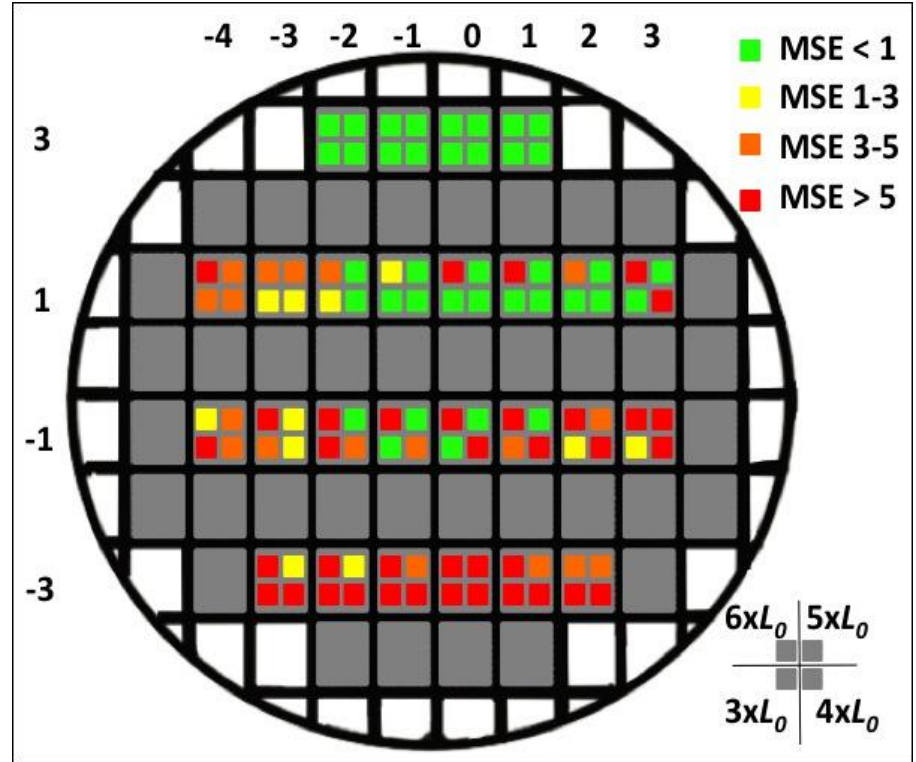


MSE value increases for all different guide pitch samples with increase in disorientation

Wafer map for PS-*b*-PMMA patterns (un-etched)

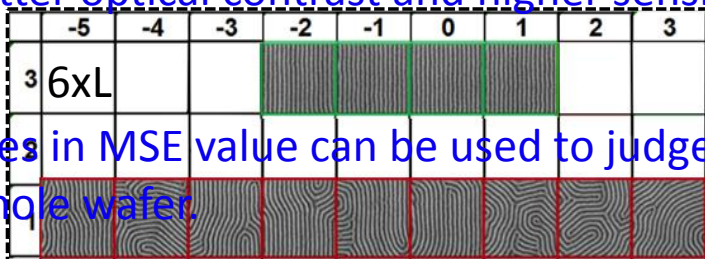


Wafer map for PS line space patterns (etched)

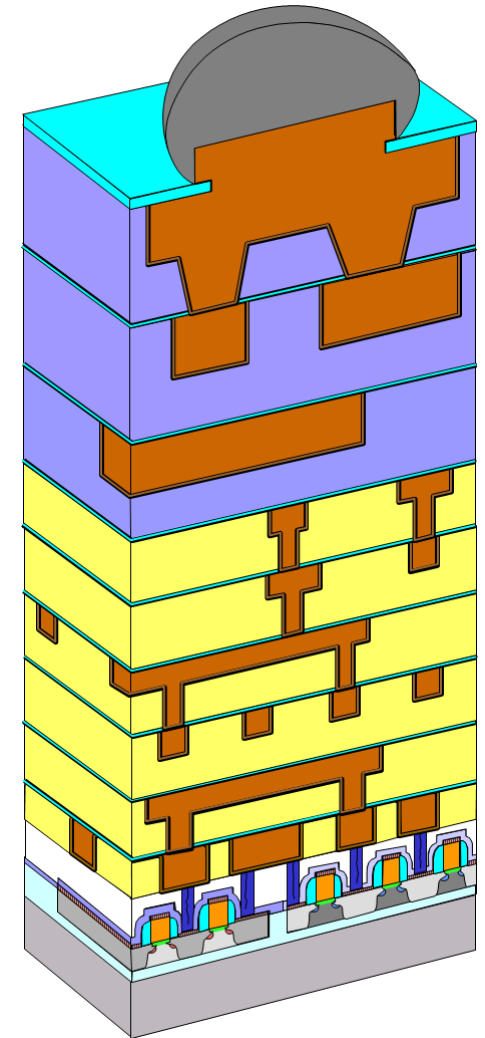


Better optical contrast and higher sensitivity for MMSE was obtained for etched samples. Wafer map with respect to MSE value.

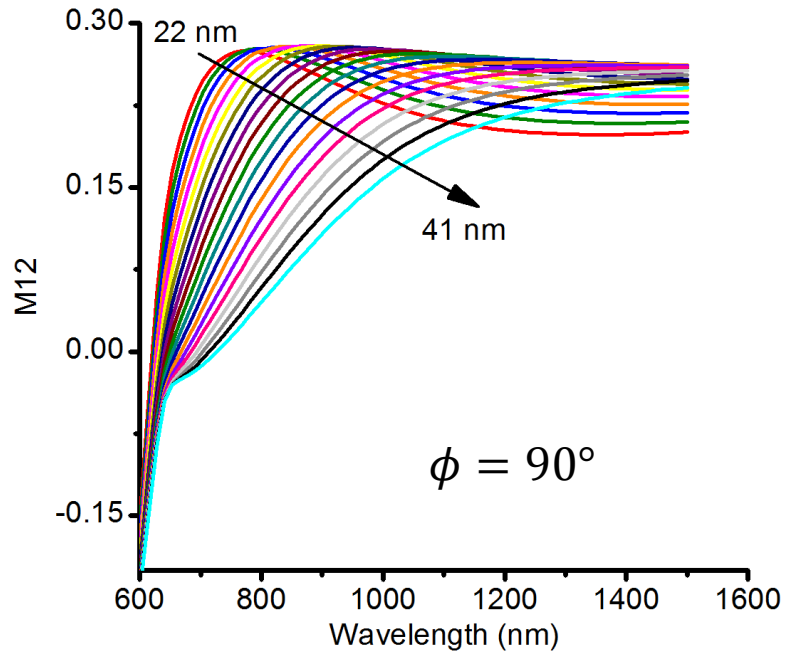
Changes in MSE value can be used to judge degree of alignment of PS line space patterns across the whole wafer.



- Challenges for interconnect technology according to ITRS:
  - Trench depth and profile
  - Via shape
  - Measure lines  $< 25$  nm wide
  - 14 nm node in production  $\rightarrow$  Metal lines  $\sim$  (25 nm width, ie  $\frac{1}{2}$  pitch)
  - Line edge roughness
- **Enhance OCD methods to overcome insensitivity to changes in metal line CD and shape**



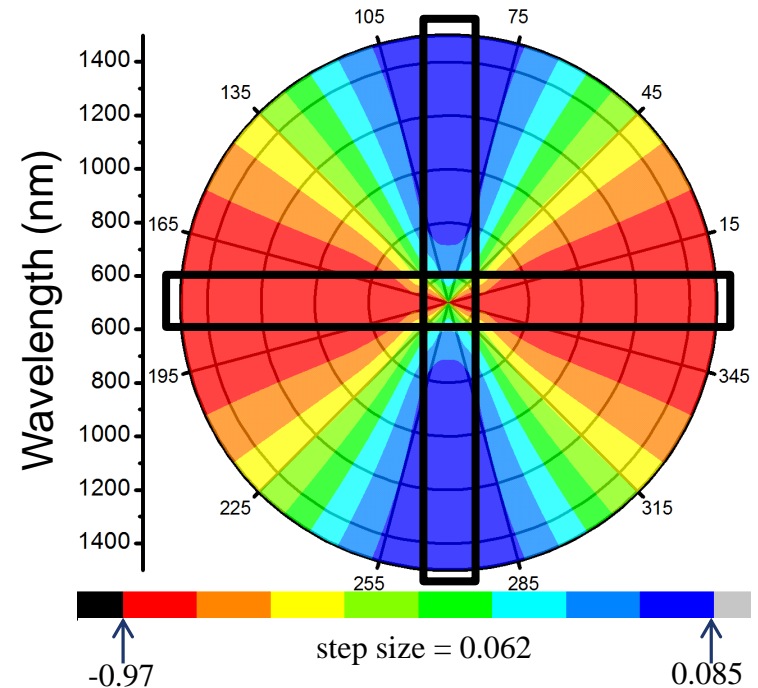
M12: CD variation 1D Cu lines AOI = 65°



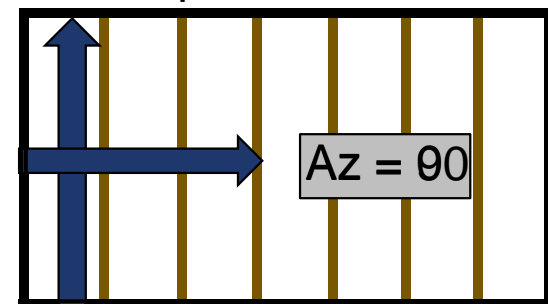
$$M_{12} = -\cos(2\gamma)$$

- Poor sensitivity to CD / No characteristic minima
- No Plasmons for small CD grating at  $\phi = 0^\circ$
- **~1 nm CD sensitivity**
- Pitch is 64 nm in left plot

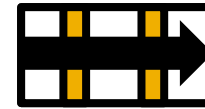
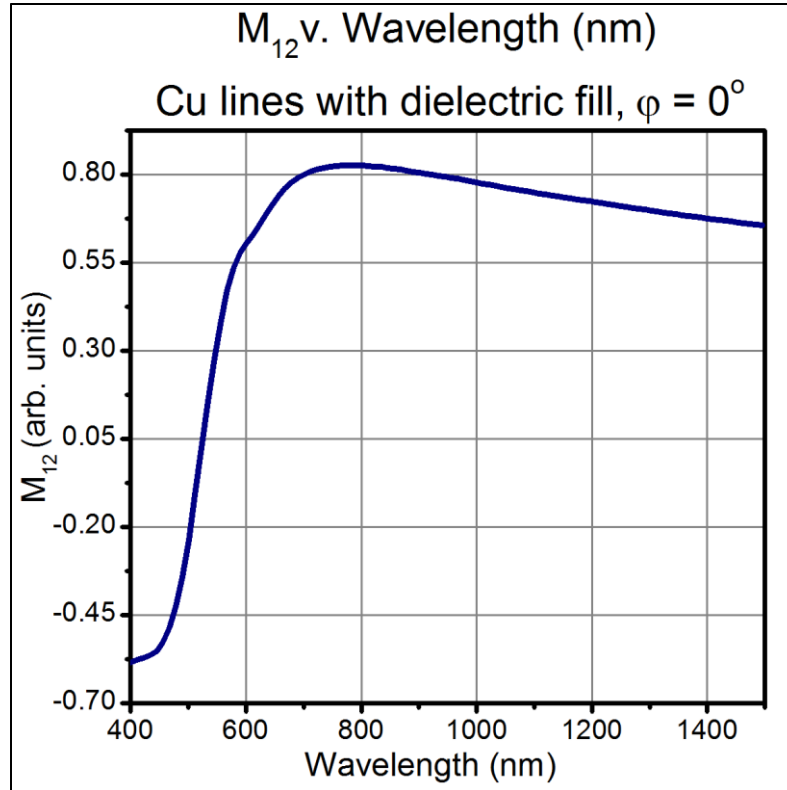
M12: Azimuthal rotation v. wavelength



Top Down View



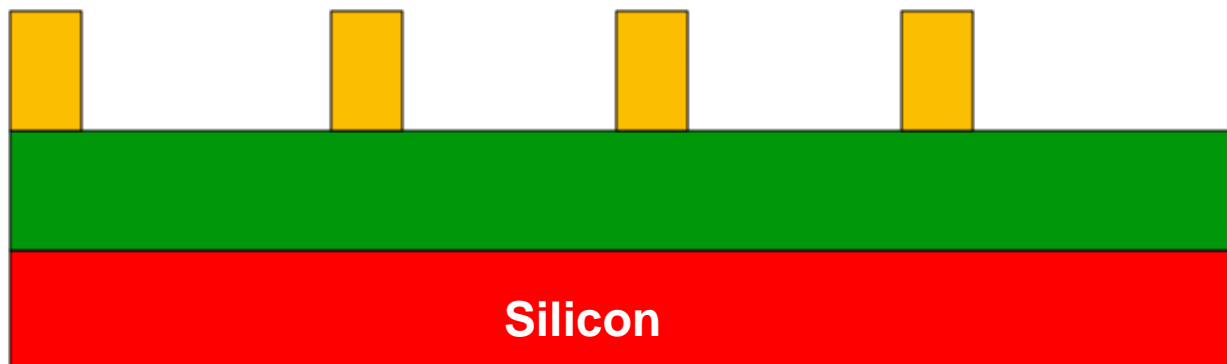




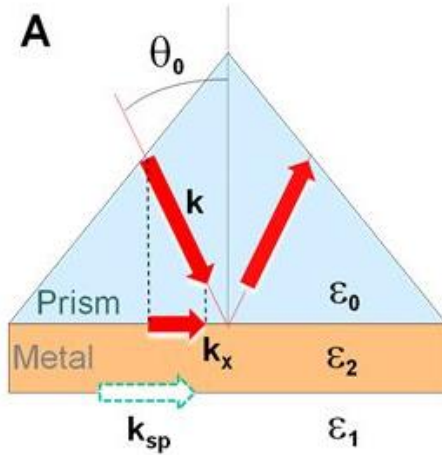
$P_x = 120 \text{ nm}$

Azimuthal angle relative to small Cu lines

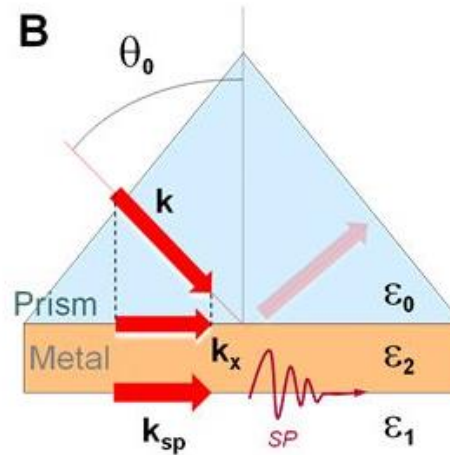
- Left: minimally distinguishable curves for  $CD_Y = 18 - 30 \text{ nm}$  with a 2 nm step size
- Largely featureless in IR-visible wavelength range
- Azimuthal angle change has minimal effect on CD sensitivity



CD	
◆	18 nm
◆	20 nm
◆	22 nm
◆	24 nm
◆	26 nm
◆	28 nm
◆	30 nm

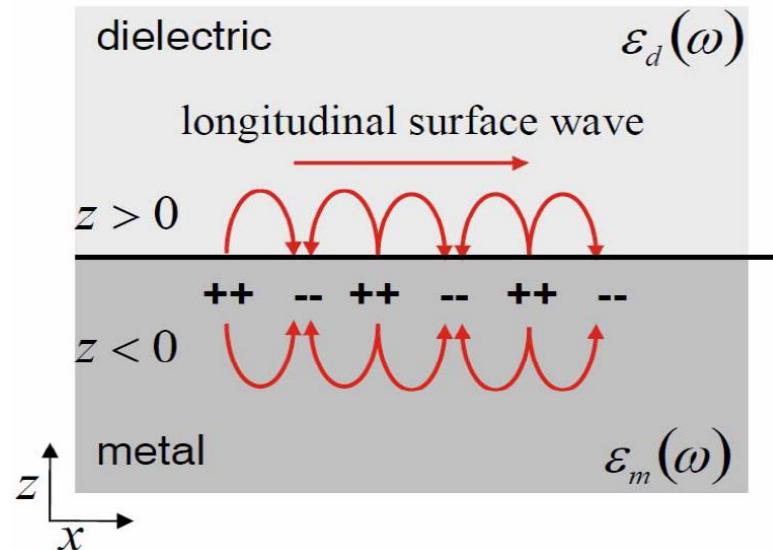
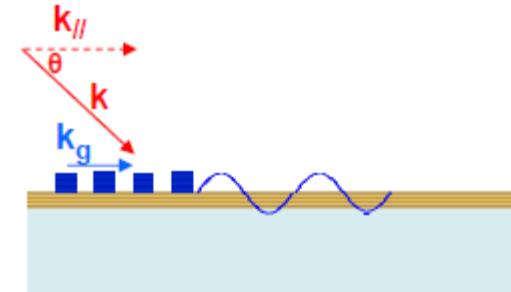


$k_x \neq k_{sp} \rightarrow$  No plasmon excitation



$k_x = k_{sp} \rightarrow$  Plasmon excitation

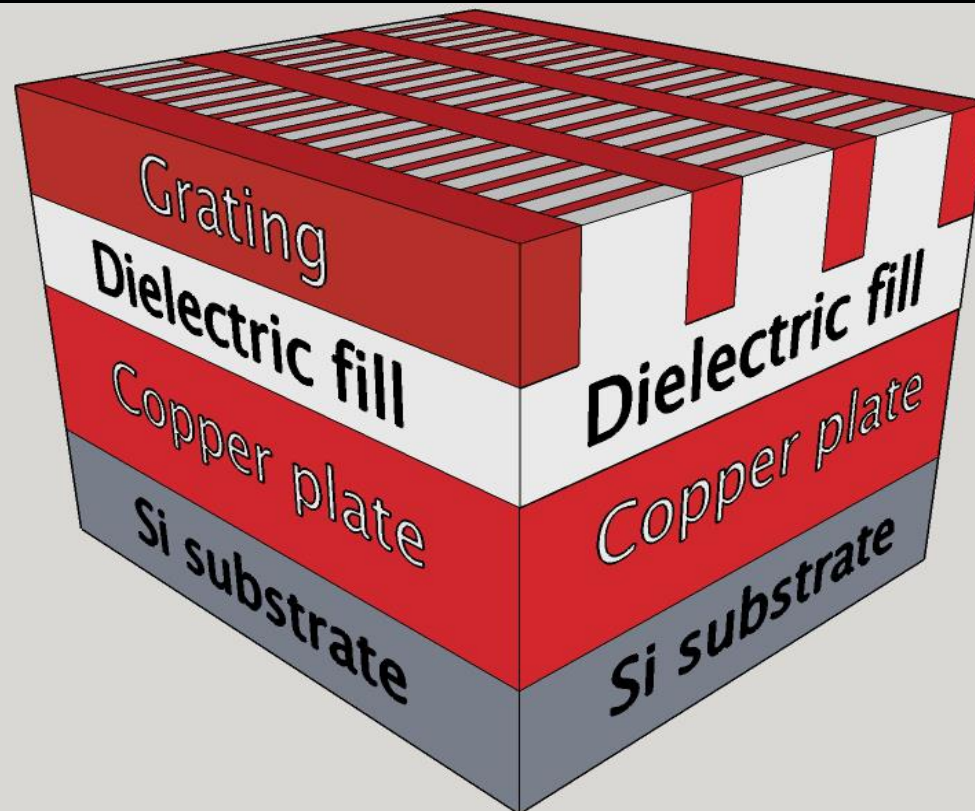
### Coupling to a grating



**Surface Plasmon Polariton  
Transverse Magnetic Mode  
Also called p mode**

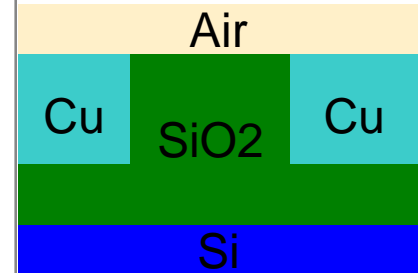
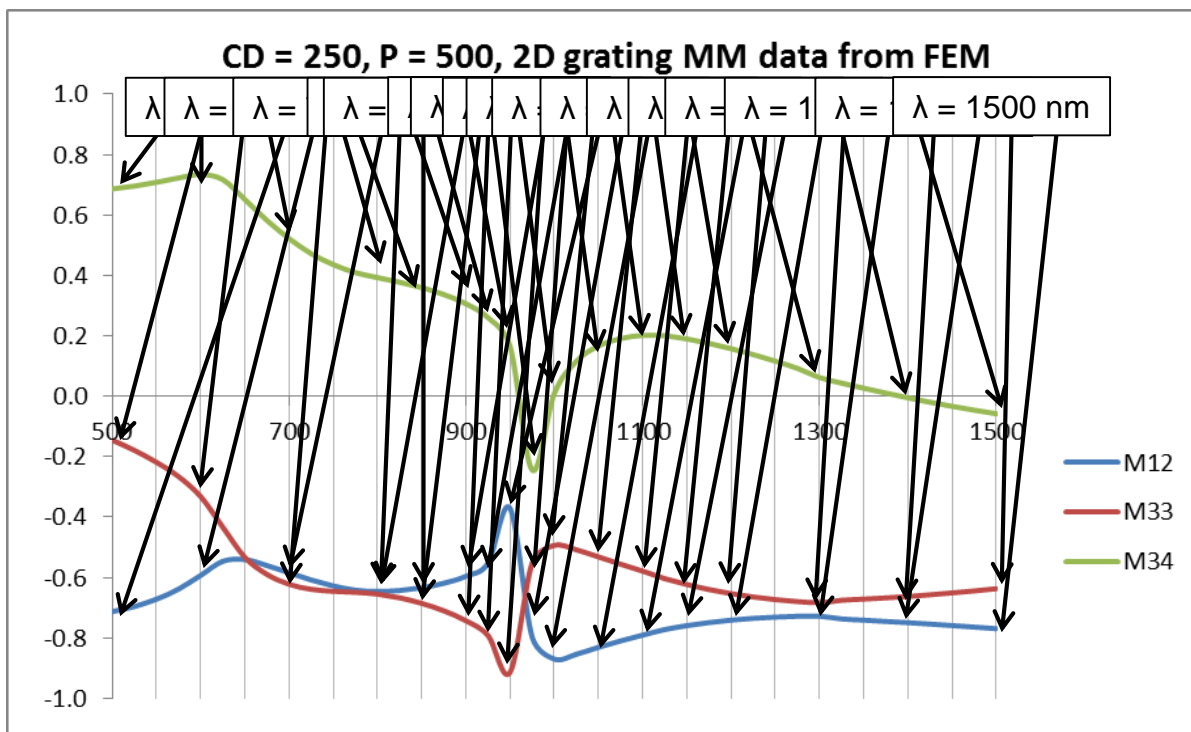
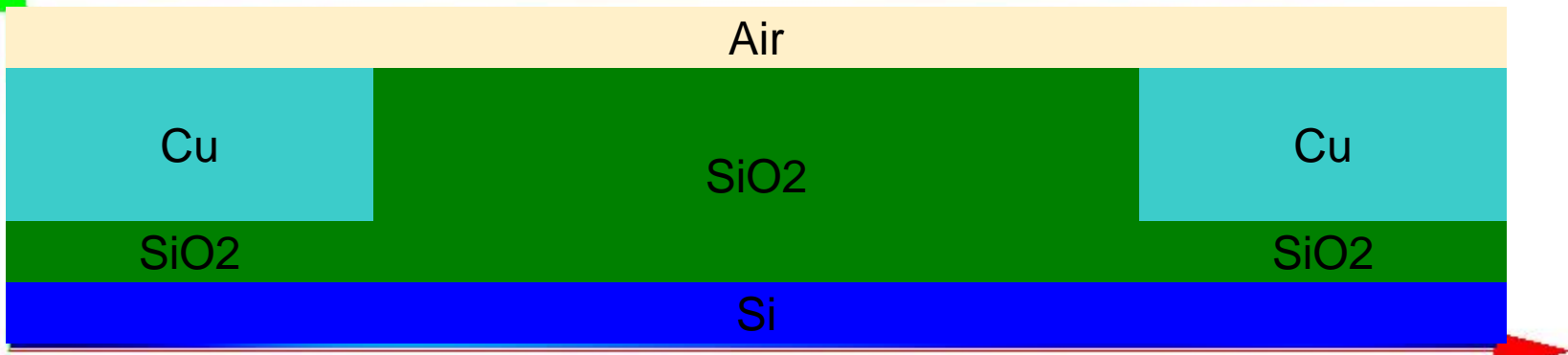
[https://www.photonics.ethz.ch/fileadmin/user\\_upload/Courses/NanoOptics/plasmons2.pdf](https://www.photonics.ethz.ch/fileadmin/user_upload/Courses/NanoOptics/plasmons2.pdf)

- Picture below: 3D views of structure
- Use larger features to launch plasmons that enhance sensitivity to smaller features

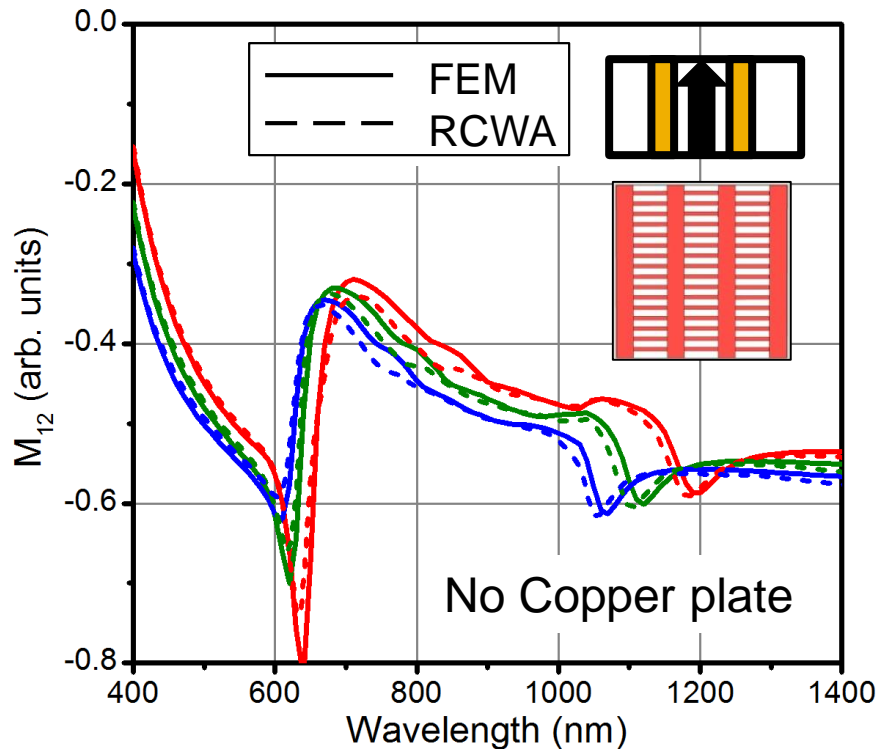


- Convergence difficulty for RCWA simulation of metallic cross-grating
  - Requires more computational power than local computer provides
  - Solved with new NanoDiffract engine and cloud based computing
  - Many publications on plasmonic-sample ellipsometry attempt to model only key spectral features with RCWA, often poorly due to above considerations
  - Our work can model entire spectra with RCWA+FEM approach
- FEM time constraints
  - 1 simulation = 1-10 minutes comp. time, 1 spectra = 2-10 hours
  - Depends on sample parameters (mesh, sample volume) and wavelength step size
  - All simulations run locally, no cluster computing

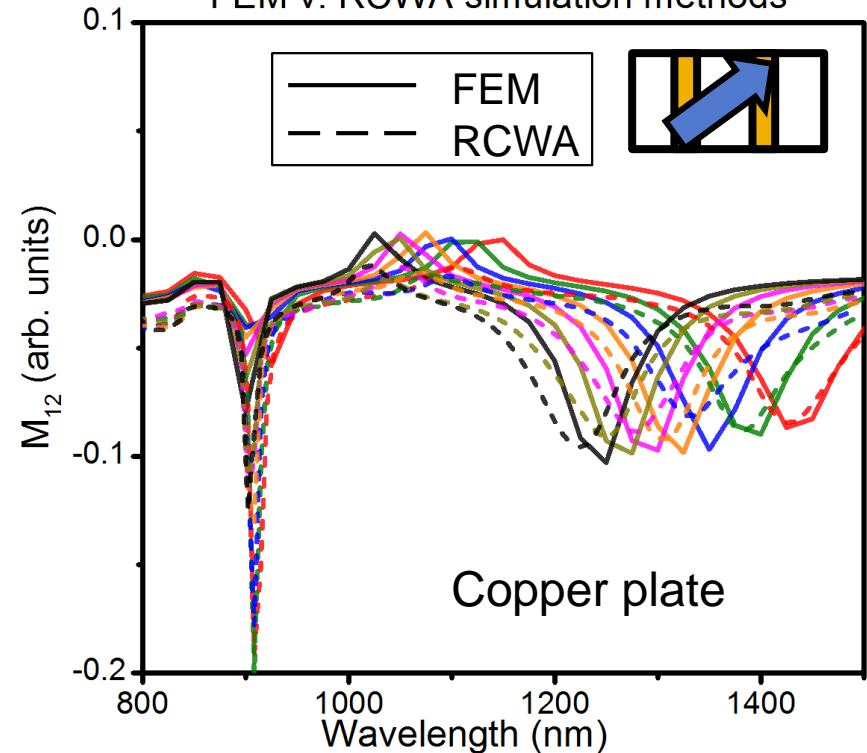
H field color range: red = 50  $\mu$ A/m, blue = 0  $\mu$ A/m



$M_{12}$  v. Wavelength (nm),  $CD_Y = 8-12$  nm,  $T_p=0$   
 $\varphi = 90$  degrees, FEM v. RCWA simulation methods

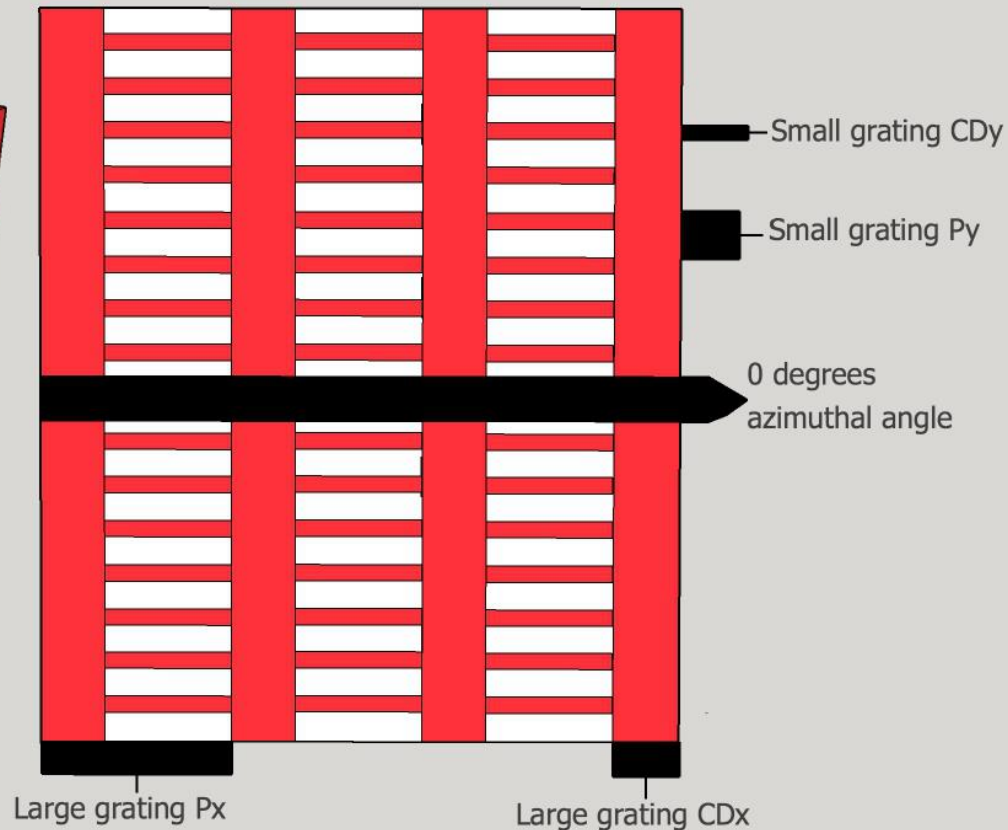
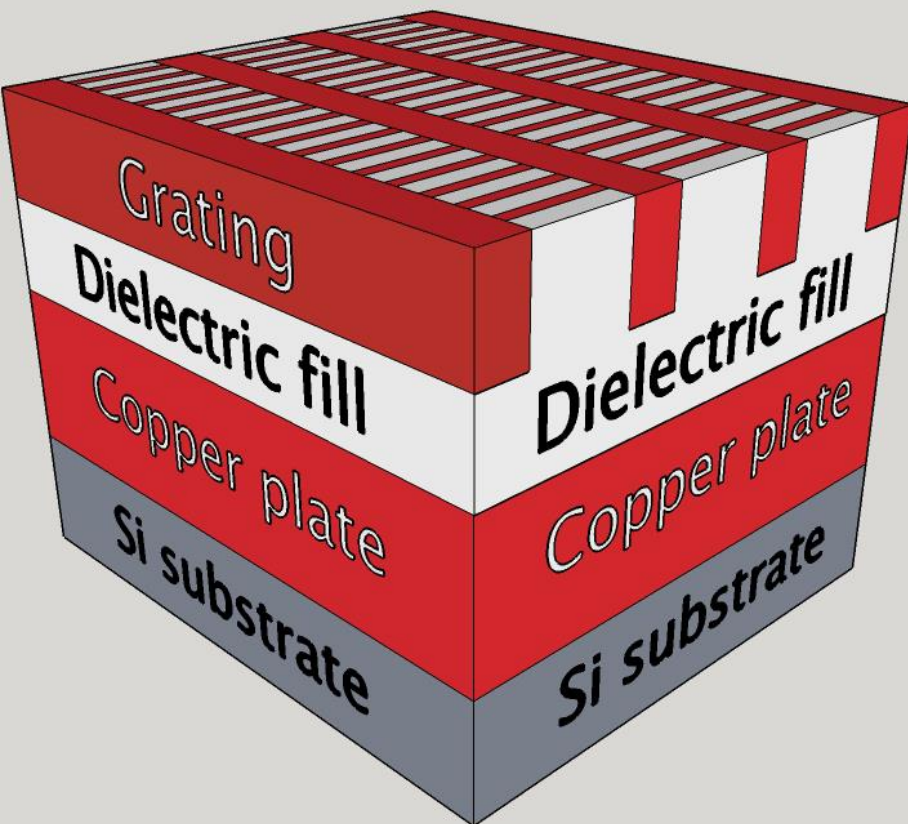


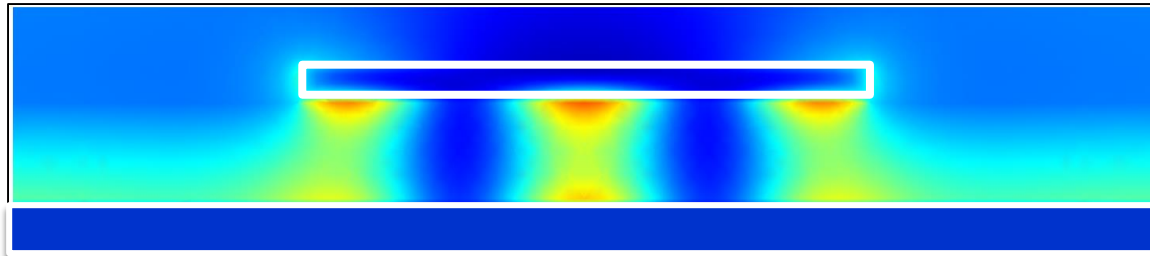
$M_{12}$  v. Wavelength (nm),  
 $CD_Y = 18-30$  nm,  $\varphi = 45$  degrees  
 FEM v. RCWA simulation methods



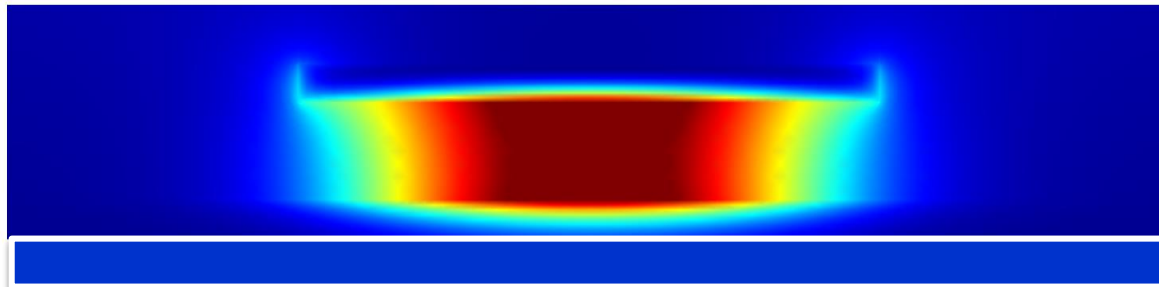
- Left: original cross-grating, red  $CD_Y = 8$  nm to blue  $CD_Y = 12$  nm
- Right: new cross-grating (w/Cu plate), red  $CD_Y = 18$  nm to blue  $CD_Y = 30$  nm

- Picture below: 3D and top-down views of structure
- Use larger features to launch plasmons that enhance sensitivity to smaller features



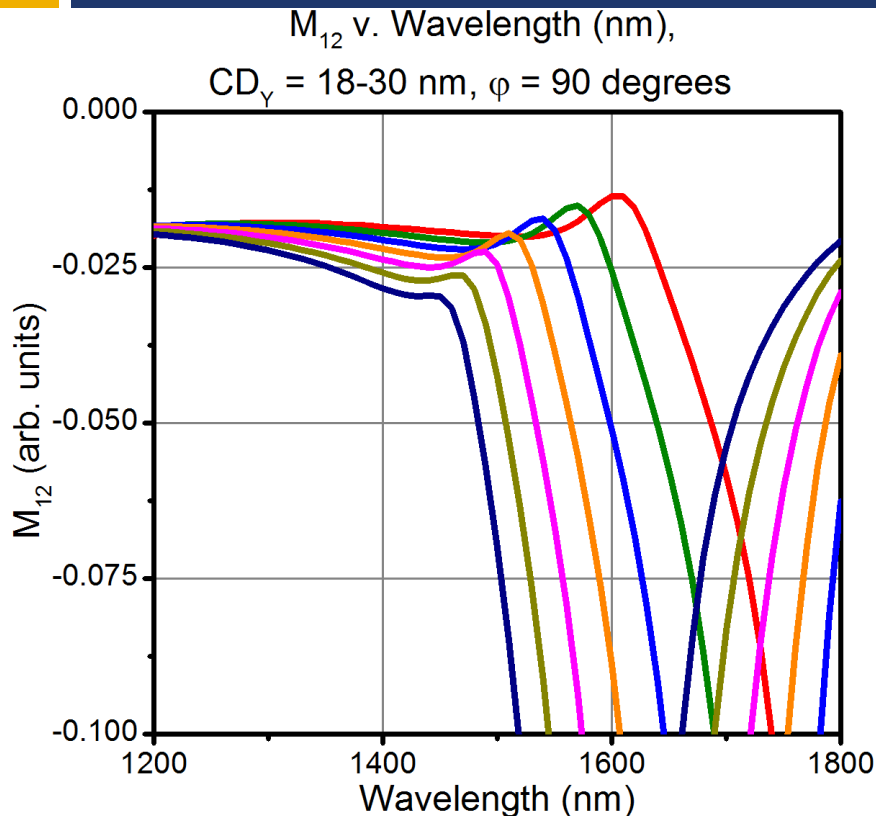


H field for cross-grating structure,  $\phi = 0$ ,  $\lambda = 700$  nm.  
 Dark blue  $H = 0$   $\mu\text{A/m}$ , red  $H = 50$   $\mu\text{A/m}$ . Localized plasmon activity in between copper grating (white outlined rectangle) and copper plate (substrate seen).



H field for cross-grating structure,  $\phi = 0$ ,  $\lambda = 1450$  nm.  
 Dark blue  $H = 0$   $\mu\text{A/m}$ , red  $H = 50$   $\mu\text{A/m}$ . Localized plasmon activity in between copper grating and copper plate.

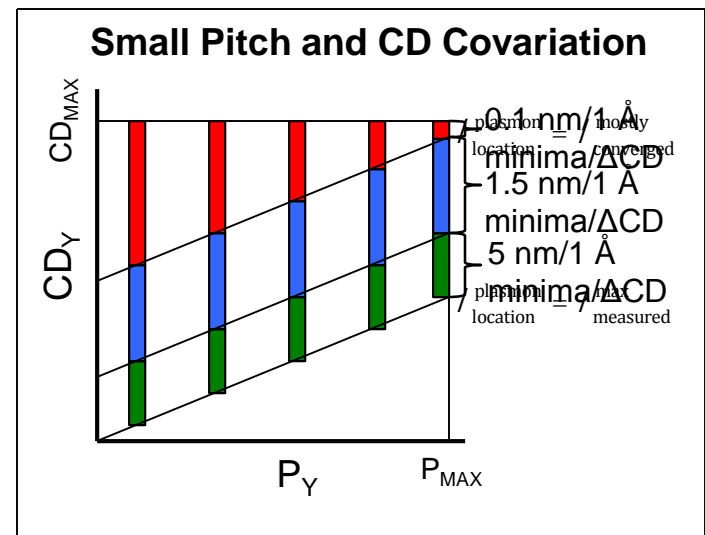
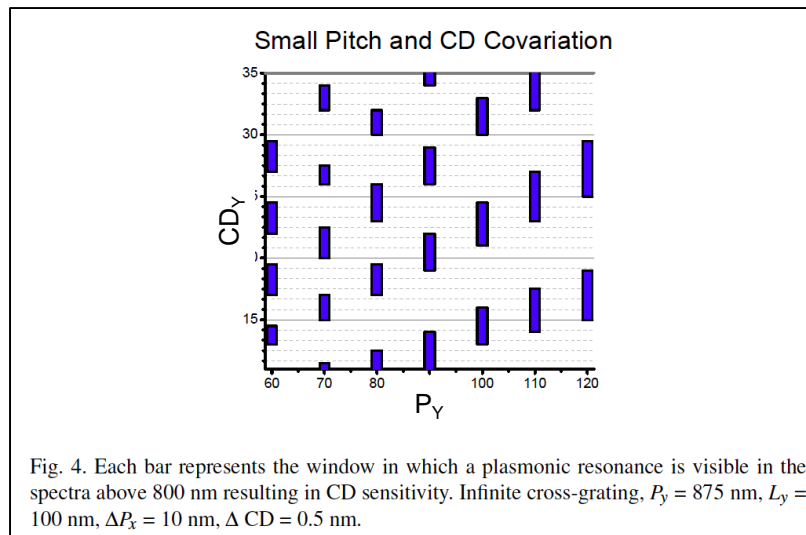




- CD<sub>Y</sub> variation from 18 to 30 nm with a 2 nm step size
- $M_{12}$  spectra shown
- Two distinct minima: first between 1600-1800 nm and second between 900-1100 nm
- Maxima from 850-950 nm and 1450-1600 nm
- SPR at 700 nm
- $P_Y = 120$  nm;  
CD<sub>X</sub> = 100,  $P_X = 600$  nm

➤ Fill-factor (old assumption)

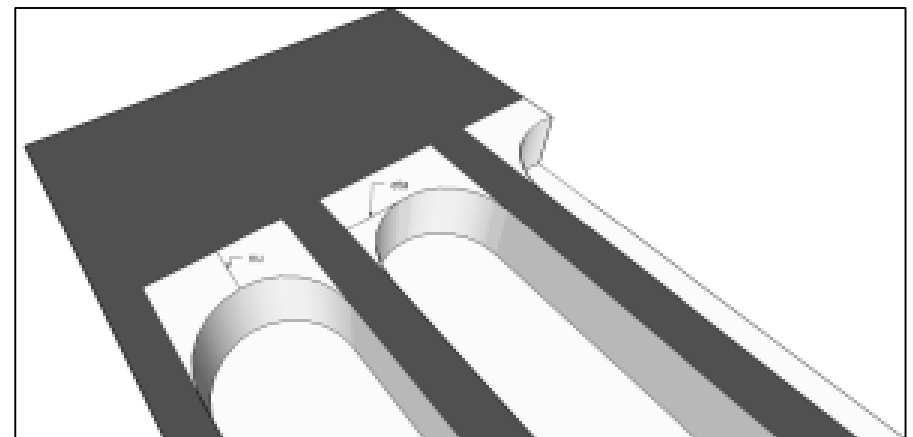
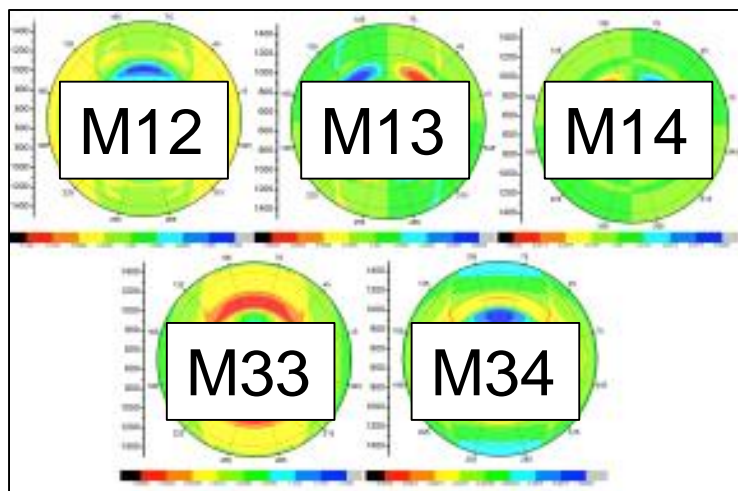
- Localized minima location highly dependent on the area ratio  $\frac{A_{grating}}{A_{total}}$
- Result: increasing CD leads to **higher order** localized plasmons (left)



➤ Relative-CD (new observed behavior)

- Localized minima location highly dependent on the change  $\frac{DCD}{CD_{nominal}}$
- Result: increasing CD leads to **convergence** towards single minima (right)
- Higher orders normally present in visible spectra, coexist with primary minima

- Using FEM for initial analysis important for accurate modeling of resonant structures
- Combined FEM+RCWA method guarantees quick modeling capabilities with accurate results
- **Fabricated Samples will have rounded edges**



**Prolith Simulation**

Difference between rectangular and rounded

- Nanometrics (RCWA simulator, funding)
  - ▣ Nick Keller
  - ▣ Joseph Race
- JCMWave (FEM simulator)
  - ▣ Sven Berger
- Prof. Diebold's optical physics group @ SUNY CNSE
  - ▣ Avery Green
  - ▣ Yong An
  - ▣ Sonal Dey



Manasa Medikonda  
Raja Muthinti  
Dhairya Dixit  
Sam O'Mullane  
Florence Nelson  
Avery Green

Steve Consiglio  
Kanda Tapily  
Gert Leusink

Brennan Peterson  
Andy Antonelli  
Nick Keller

Mathew Wormington (Jordan Valley now Bruker)



GRC



This work is sponsored in part by INDEX, a funded center of NRI, a Semiconductor Research Corporation (SRC) program sponsored by NERC and NIST.